Defensible Resource Allocation for Plant Health Surveillance: Optimal Border and Post–Border Surveillance Expenditures

Tom Kompas
Centre of Excellence for Biosecurity Risk Analysis
University of Melbourne

Long Chu, Pham Van Ha and Hoa Thi Minh Nguyen
Crawford School of Public Policy
Australian National University

Susie Collins and Ranjith Subasinghe
Department of Agriculture and Water Resources
Canberra, Australia

November 2017

CEBRA PROJECT 1608A
DEFENSIBLE RESOURCE ALLOCATION FOR PLANT HEALTH SURVEILLANCE

CENTRE OF EXCELLENCE FOR BIOSECURITY RISK ANALYSIS (CEBRA)
UNIVERSITY OF MELBOURNE

Contents

List of Figures

List of Tables

1 Executive Summary

Biosecurity agencies face challenging decisions of how best to allocate scare resources when they attempt to prevent, detect, eradicate and suppress exotic and established pests and diseases. In this regard, there is a key difference between the value of biosecurity measures and the extra value, or value-added, of investments in biosecurity. The overall question, in other words, is not how valuable a given biosecurity measure (or set of measures) is, but how to allocate resources across different biosecurity measures and threats to get the best possible rate of return.

While resource allocation in biosecurity may be approached as a standard portfolio problem (Akter et al., 2015), allocating resources to address biosecurity threats may pose three additional challenges. First, policy makers are often faced with a (possibly large) number of pests, and each can be associated with a range of biosecurity measures, namely pre-border, border quarantine, post-border surveillance, and containment and eradication. A measure to control or prevent a particular pest likely influences the effectiveness of other measures, and the overall cost-effectiveness of the money spent to address this problem. Consequently, a biosecurity portfolio must allocate a budget not only across different pests, but also across different measures to detect and control them. Second, invasive species are diverse in terms of how they spread, how they cause damage and how they are controlled, so evaluating cost-effectiveness across measures and species, as well as making them comparable, is complicated. Finally, apart from the biological and ecological stochasticity inherent in invasive species that can influence the outcome (Perrings 2005), a biosecurity portfolio must often be decided at early stages where information about many of the characteristics of the threats are very rough and scant. For this reason, biosecurity portfolio models ideally should not be overly demanding in the information required to calibrate them.

A proper portfolio allocation in biosecurity differs from the common principle which ranks alternative projects by their benefit-cost ratios (Pearce et al., 2006) and picks the one that generates the highest benefit-to-cost ratio (BCR). This principle is sometimes referred to as 'the winner takes all' principle because the projects with highest average BCRs will be allocated at full scale while others may have no budget. This often results, however, in a misallocation of resources because the average BCR of a biosecurity project can be highly sensitive to its scale. Instead, it's best to allocate each (small) block of budget to the treatment and measure that it is most cost-effective, and consequently determine the optimal scale of the control program for each threat with different levels of budget constraints. The cost-effectiveness of each block of budget spent on a threat is determined by minimising its expected total cost, including the damages it inflicts and the control expenditures incurred in preventing or mitigating damages. In this way, rates of return from a given biosecurity measure are maximised. BCRs can be positive at different scales, in other words, but the key is to find the largest difference between benefits and costs.

This report, for *CEBRA Project 1608A*, illustrates these points, in terms of: (a) the optimal trade-off between border and post-border biosecurity expenditures, and (b) the optimal level of post-border 'early detection' of an exotic pest. The case we examine is papaya fruit fly (PFF) through the Torres Strait pathway, although the principles apply broadly. The border is taken

as trapping (and other) activity in the Torres Straight Islands (TSI) and post-border is defined by a surveillance measure in northern Queensland.

In terms of (a), allocations between border and post-border surveillance depend on a host of complicated issues, and a set of parameters that drive a computational outcome. That said, the idea is simple: we need to find a set of measures, at the border and post-border, that maximise rates of returns by minimising the sum of all potential damages and the cost of the biosecurity measures themselves. This is equivalent to finding an allocation that ensures that the extra benefits of combined biosecurity measures, border and post-border, in terms of all the avoided losses that go with these measures, exactly equal the extra costs of providing the measures themselves.

In this part of the report the key parameters are average arrival rates, spread rates, eradications costs, the discount rate, and the effectiveness of quarantine and surveillance measures. Using these (and other) baseline parameter values we can calculate optimal border quarantine and post-border surveillance measures. The results from the PFF case determine an overall optimal expenditure or portfolio allocation at a ratio of 1:5 for border and post-border measures. Given parameter values, in other words, and although both activities are valuable, it pays to invest more in post-border surveillance than at the border. Sensitivity results outline the range of possibilities given changes in parameter values.

In terms of (b), allocating resources for post-border surveillance, taken separately, given border quarantine measures, also generates an issue of value versus value-added or what the best rate of return should be. For a trapping network for the 'early detection' of fruit flies, for example, the question is, put simply, how early to detect a possible incursion in order to maximize the probability of eradication. A trapping grid that is very 'tight', with many traps placed in host-suitable areas will detect very early, but then the cost of the program itself, with a large number of traps, is very expensive. Having less traps means the cost of the surveillance program is lower, but then detection will be later and thus potential avoided losses will be higher. In total, if the extra benefits of adding more traps exceed the extra costs, that investment should take place, and continue to take place until extra benefits exactly equal extra costs.

In this part of the report, which modifies and extends material contained in CEBRA Project Report 1405C, *Baseline 'Consequence Measures' for Australia from the Torres Strait Islands Pathway to Queensland: Papaya Fruit Fly, Citrus Canker and Rabies*, we illustrate how to determine an optimal point of early detection. The parameter set is further complicated with control costs, production losses, the costs of trapping, and the probability of a given fruit fly to find a nearby host, among other things. Results indicate an optimal grid size of less than 1km, much less than current practice. As expected, a grid size that is much smaller than this implies that the cost of the program is too large relative to the extra benefits (in terms of the smaller avoided losses that go with early detection). A grid size that is larger than 1km generates relatively large and (otherwise) potentially avoided losses. The best grid size is illustrated by the minimum of all losses and expenditures. This maximises the rate of return from the surveillance activity. Model runs and sensitivity analysis further elaborate the role of border versus post-border biosecurity measures in terms of changes in the 'arrival rate' and its effect on expenditures.

Recommendations

1. Both the basic and the more complex spatial model in this report perform well, and clearly illustrate tradeoffs between border and post-border expenditures on biosecurity. This forms a basis for discussions of resource allocation across various biosecurity measures, and should be further developed or refined going forward.

2. Although data and estimations are available for most of what is needed, the model framework likely requires a more careful calibration of parameter values, especially in cases where model results are most sensitive to changes in these values, and where measures of 'effectiveness' of border and post-border activities are needed.

3. Pre-border expenditures could be added to the model framework, in principle, given needed data and estimates of underlying parameter values. This should be pursued going forward to allow for best 'portfolio allocations' of biosecurity expenditures across the *entire* spectrum of biosecurity measures.

2 Introduction

Along with established environmental pathways, increases in trade and tourism have increased the risk of an introduction and spread of exotic pests or invasive alien species (IAS). These pests and diseases cause enormous environmental and economic damages every year. For example, in the United States, IAS costs $137 billion yearly (Pimentel et al., 2000) and is the second most ranked threat to biodiversity, affecting 49% of imperilled species (Wilcove et al., 1998). The economic loss due to IAS worldwide is extensive, and redressing the disappointing progress made in reducing their damages to biodiversity is highlighted as one of the United Nations Millennium Development Goals (Butchart et al., 2010; Gurevitch and Padilla, 2004).

Prevention and control are the first line of defence against an IAS (Olson et al., 2006). They absorb significant resources. For instance, about $40 billion is spent each year on global pesticide expenditures (Grube et al., 2011), while almost 50% of national expenditures for IAS are for prevention activities (NISC, 2001). Spending on prevention and control alone is not economically effective, however, since: (a) complete prevention has often proven to be impossible and prevention measures, no matter how stringent they are, cannot keep up with the increasing risks of a bio-invasion due to globalisation (NISC, 2008) and new or enhanced environmental pathways; and (b) although the chance of a successful invasion by an IAS is often small (Williamson, 1996), these threats, once established, are usually very expensive if not impossible to control unless their presence is detected early (Sinden et al., 2004; Clark and Weems Jr, 1988). For these reasons, early detection and rapid response (EDRR), the second line of defence, has attracted considerable attention over the last decade, with a particular focus on the trade-off that exists between the early detection of an IAS and the future cost of controlling it (Mehta et al., 2007).

The challenge of finding an optimal early detection point or the appropriate surveillance level depends on the economics of the problem and how an IAS invades and spreads. In general, there is a good deal of uncertainty over the likelihood of an incursion, its spread in terms of spatial and temporal characteristics (Kot et al., 1996; Shigesada and Kawasaki, 1997; Keeling et al., 2001), and the potential economic damages that might occur. The model context is also necessarily large in this case, and fully and explicitly considering time, space, uncertainty and variability in economic damages in an optimisation problem quickly leads to 'a curse of dimensionality' (Bellman, 2003) and computational failure.

This report, for *CEBRA Project 1608A*, contains two different (but related) model approaches. The first approach presents a practical model which can help government agencies allocate a biosecurity budget to where it is most cost-efficient. To evaluate the cost-effectiveness of a single invasive, we draw from a generic framework, first proposed by Moore et al. (2010), which focuses only on the most common economic features of biosecurity measures associated with all invasive species, namely (a) quarantine against entry risk and (b) surveillance against late-detection treatment, loss and inability to eradicate. However, we include two major ex-

tensions. First, our model makes endogenous the costs of failed quarantine and detection by allowing them to vary with a number of some fundamental factors such as the spread rate, damage rate and eradication cost per one infected unit. Second, we model the detection probability as a function not only of the surveillance expenditure, but also the size of infestation to better reflect the fact that some threats could be detected with no active surveillance if they grow bigger and bigger. Both extensions aim at enhancing the practicality of the model while requiring a few, albeit largely indispensable, parameters which can be estimated or collected by policy makers or adopted from relevant sources.

Given various border measures, the second approach aims to directly find the optimal level of surveillance against fruit flies, post-border, in a more complicated spatial setting. This surveillance problem is particularly challenging since not only do fruit flies disperse quickly in a highly random manner in a local environment, as well as over long distances, they have a rate and, to a lesser extent, direction of dispersal that is also largely dependent on time and environmental factors (Yonow and Sutherst, 1998). Among the biggest challenges in this kind of problem is the possibility of numerous invasions, across space and time that fruit flies can make throughout their life cycle, and especially the fact that it is impossible to guarantee any particular outcome with certainty. All of these features make the simulation of this IAS dispersal exceptionally difficult, let alone finding the optimal surveillance measure against them.

The surveillance model we develop here is a stochastic spatial dynamic bio-economic model. With this model, we examine explicitly time, spatial heterogeneity, uncertainty and the variability of economic damages. Applied to the case of Asian Papaya Fruit Fly (PFF) (*Bactrocera papayae*) in the state of Queensland, Australia, the random dispersal of PFF is calibrated to mimic the first PFF outbreak in north Queensland in November 1995. Furthermore, the spread of PFF is modelled using a highly detailed (50m$\times$50m) raster map on land use, while the historical seasonal spread features of fruit flies are fully incorporated. To find the optimal surveillance to detect PFF early, we use a Sample Average Approximation (SAA) approach combined with a parallel processing technique to handle dimensional complications. We are not aware of any other applications of this large dimension modelling in environmental and biosecurity economics.

3 Related Literature

Time, space and uncertainty being considered fully and explicitly in an optimisation routine is generally limited by the curse of dimensionality. To make the problem manageable, early studies on optimal surveillance against an invasive threat often reduced the problem to one or two dimensions, with spatial heterogeneity either ignored (e.g. Mehta et al., 2007; Bogich et al., 2008), or largely reduced in dimension (Sharov, 2004; Ding et al., 2007; Finnoff et al., 2010a; Blackwood et al., 2010; Sanchirico et al., 2010; Gramig and Horan, 2011; Kompas et al., 2016). Since an IAS spread is highly dependent on spatial heterogeneity, this 'aggregate' approach can produce misleading results (Wilen, 2007; Albers et al., 2010; Meentemeyer et al., 2012). As a second alternative, some studies opt to neglect the time dimension and thus optimise surveillance effort at a single point in time (Hauser and McCarthy, 2009; Horie et al., 2013) or at a steady state (Epanchin-Niell et al., 2012a). The main concern with this approach is that the solution it generates is not likely optimal for the entire time path, or it may generate a solution for a steady state which might be reached only very slowly or never be attained (Finnoff et al., 2010b). A third approach to IAS modelling (Epanchin-Niell and Wilen, 2012), is to explicitly model both time and space, but in a deterministic setting, thereby no longer allowing for fully articulated surveillance problems where uncertainty over spread, space and time matters. When there is uncertainty in whether an incursion occurs, or whether an (unknown) incursion can be detected early, or potentially eradicated, (Barnes, 2016; Robinson, 2002; Sivinski et al., 2000),

decisions on border and post-border measures must take into account possibilities that can be realised at different points in time.

For the spread of most IAS, time, spatial characteristics, uncertainty and variability in damages all play important roles that should not be ignored. For this reason, the literature on some plant diseases and trans-boundary animal diseases (TADs) relies mostly on simulations, without an optimisation routine, to fully and explicitly model all of these dimensions (Morris et al., 2001; Ferguson et al., 2001; Tomassen et al., 2002; Keeling et al., 2003; Tildesley et al., 2006; Ward et al., 2009; Adeva et al., 2012; Hayama et al., 2013; Atallah et al., 2014). Simulations, however, reveal only the relative efficiency of one, or at best, a limited number of policy choices.

To address this shortcoming of simulation methods, a simulation-based optimisation approach has been proposed recently. The idea of this approach is to keep the spatial dimension manageable by capturing only the 'average' movements of IAS over space (Kobayashi et al., 2007; Kompas et al., forthcoming). While providing useful insights, this approach would likely loose some spatial heterogeneity in spread patterns during the process of estimating transmission coefficients.

To solve large-dimensional optimal surveillance problems explicitly, Kompas et al. (2015) use a Sample Average Approximation (SAA) method in surveillance problems for TADs. Having desirable asymptotic statistical properties, SAA solves stochastic dynamic problems by using a combination of exterior sampling and deterministic optimisation (Shapiro et al., 2014; Shapiro, 2003; Verweij et al., 2003). To make SAA amenable to surveillance problems for TADs, we design an infection tree model focusing on infection paths, not infectious farms, and implement sensible 'pruning' rules to substantially reduce the dimension of the problem, which in turn is solved with the aid of parallel processing techniques. However, this innovation is not directly applicable to surveillance problems for IAS that can fly, since these species can make numerous contacts and invasions throughout their entire lives, thereby making the proposed infection tree infeasible to build due to its enormous dimension. Moreover, these IAS can hardly be traced or contained, making any pruning rules difficult. Given these modelling challenges, the literature on optimal surveillance against these IAS is extremely scant and largely ignores the spatial dimension (Pierre, 2007; Kompas and Che, 2009; Florec et al., 2013).

We aim to solve this problem, making two important contributions to the literature. First, the random dispersal of PFF in our model is calibrated based on a highly detailed 50m×50m land use raster map with up to 1.4 billion cells, and historical incursion and spread data together with information on seasonal spread patterns. Second, we solve a large-dimensional optimal surveillance problem with an adaptation of the SAA approach in combination with parallel processing, while still retaining complex spatial and time dimensions, and fully incorporating uncertainties. Few optimisation problems of this dimension have been solved in environmental and biosecurity economics to the best of our knowledge.

4 Papaya Fruit Flies and Study Area

Fruit flies are a major threat to horticultural crops in many parts of the world. They can cause profound economic losses and are difficult and expensive to eradicate. For instance, in the United States, the potential damages caused by the Mediterranean fruit fly (*Ceratitis capitata*) are estimated to be roughly $15 billion if left uncontrolled (Hagen et al., 1981), while its eradication cost in a first campaign in Florida was $7.5 million in 1930 (Clark and Weems Jr, 1988). In Africa, the annual damage from fruit flies is worth millions of dollars (National Research Council, 1992)[1]. Indeed, more than 50% of Africa's horticultural production is affected by fruit

[1]Billah et al. (2015) provides a thorough review of the pest status, economic impacts and management of fruit-infesting flies in Africa

fly infestations (World Bank, 2008; Billah et al., 2015), while this sector employs directly and indirectly more than 40 million people, many of whom are poor. In like manner, fruit flies cause substantial losses in many poor developing countries by affecting their export potential (Allwood et al., 1997). To this end, successful management of fruit flies will help reduce poverty, enhance food security, provide employment to poor people and foreign exchange to poor developing countries.

There are two reasons why we choose the state of Queensland (QLD) in Australia as the case study for our analysis. First, QLD and Australia are under a constant threat of PFF since PFF is native to and widespread in South-East Asia and in many of the Pacific Island Countries (Allwood et al., 1997). As seen in Figure 1 with monsoonal winds in the wet season, PFF can also 'travel' though the Torres Strait Islands (TSI), just north of mainland Australia, to QLD, along environmental and human-assisted pathways (Kompas and Che, 2009). Until now, an ongoing and strong surveillance and trapping program in the TSI has largely prevented PFF from travelling to the mainland of Australia. Eradication of detected fruit flies occurs regularly in the TSI and local traps in QLD can potentially detect PFF early should it escape the quarantine and surveillance zones in the Torres Strait (DAFF, 2005). However, the threat to QLD and Australia from PFF remains high with estimates of the damages of a country-wide spread of PFF being $AUD 3.3 billion over a hundred year horizon (Hafi et al., 2013). The first outbreak in QLD 1995 cost $AUD 34 million and took over four years to eradicate (Cantrell et al., 2002). The second reason is that a rich data set is available to construct a detailed stochastic spatial dynamic bio-economic model to find the optimal level of surveillance against PFF. As a result, lessons learnt from this analysis could be useful for other countries and regions, and especially for developing countries where this sort of analysis is yet to be feasible.

Figure 1: Study area: Queensland, Australia

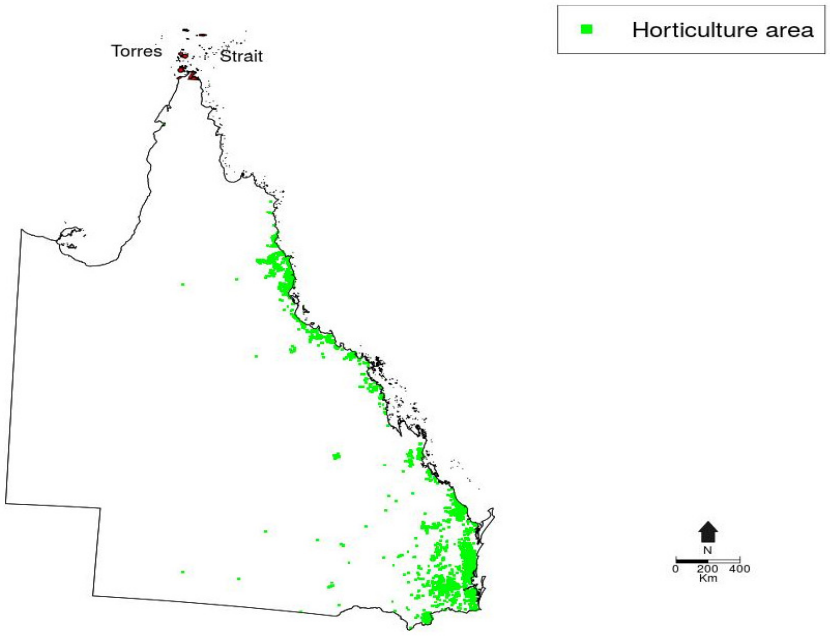

5 Pre and Post-Border Control from a Macroeconomic Perspective

5.1 Economic modelling of pre- and post-border control of PFF

We begin with the more basic and practical model, to explicitly pick up both border and post-border measures. The more fully articulated spatial model is contained in Section 6.

We model the incursion of PFF with a random-walk process $b_1, b_2 \ldots$, with b_i being the time of the i^{th} incursion. The drift, and possibly the variance, of the random walk can be controlled via prevention or quarantine. Prevention measures that reduce the frequency of incursions, including border and local quarantine, search, the removal of potential threats (including the removal of exotic species that have not yet become established), and containment of existing threats to avoid long distance dispersal (if any). Increasing the budget share allocated to prevention measures (q) will, on average, reduce the frequency of incursion or (equivalently) increase the duration of intervals between two consecutive incursion events. This implies that:

$$b_i = b_{i-1} + \Phi(q) + \varepsilon_i \tag{1}$$

where $\Phi(q)$ is the average interval between two consecutive incursions which increases with the quarantine budget q (mathematically $\frac{\partial \Phi}{\partial q} > 0$ implying that stricter quarantine measures will reduce pest entries and hence incursion probability); $\varepsilon_i \overset{iid}{\sim} D$, a random distribution with mean zero; and, for the sake of notational simplicity, $b_0 \equiv 0$.

Conditional on the incursion at time b_i, PFF spreads at rate r, so the infestation size at any time t from the entry on ($t \geq b_i$) can be represented with an exponential function:

$$x_i(t) = \widetilde{x} e^{r(t-b_i)} \tag{2}$$

where $\widetilde{x}$ is the entry size. The larger is an infestation and/or the greater the active surveillance effort, the more likely PFF will be detected. The detection probability function, denoted as $p(x, s)$, with s being active surveillance expenditure and x being infestation size when detected, satisfies the following assumptions:

$$\forall (x, s) : p \in [0, 1]; \frac{\partial p}{\partial s} \geq 0; \frac{\partial p}{\partial x} \geq 0; \forall s : p(0, s) = 0 \tag{3}$$

Conditional on being detected at size x_i, PFF will be eradicated at a (current value) cost of C per infected unit. This may not be a one-off item, as eradication might not be always successful within a campaign, but can be a flow of expenditures spent on physical removal, monitoring and other follow-up as well as repeated activities. Summing over all entries, the expected eradication cost (discounted to time zero with an annual discount rate ρ) is:

$$B_e = E\left\{\sum_{i=1}^{\infty} C x_i e^{-\rho t(x_i)}\right\} = E\left\{\sum_{i=1}^{\infty} C \widetilde{x} e^{(r-\rho)(t(x_i)-b_i)-\rho b_i}\right\}$$

$$= \sum_{i=1}^{\infty} C \widetilde{x} E\left\{e^{-\rho b_i}\right\} \int_{\widetilde{x}}^{\infty} e^{(r-\rho)[t(x_i)-b_i]} \frac{\partial p(x_i, s)}{\partial x_i} dx_i \tag{4}$$

$$= \frac{E\left\{e^{-\rho \varepsilon_i}\right\} \times e^{-\rho \Phi(q)}}{1 - E\left\{e^{-\rho \varepsilon_i}\right\} \times e^{-\rho \Phi(q)}} C \widetilde{x} \int_{\widetilde{x}}^{\infty} e^{(r-\rho)[t(x_i)-b_i]} \frac{\partial p(x_i, s)}{\partial x_i} dx_i$$

where the detection time $t(x_i)$ is the inverse function of (2).

Equation (4) shows how the eradication cost relates to prevention and active surveillance expenditures. The first fraction on the right hand side of the equation captures two possible effects of prevention, one on the incursion frequency and the other on the uncertainty over incursion time. The first effect unambiguously specifies that allocating an increased budget share to prevention will reduce the frequency of incursion and hence reduce eradication cost. The second effect of prevention is its potential influence on uncertainty over incursion times, which can only be calculated with a specific functional form for the uncertainty distribution (i.e., D).

The remainder of the right hand side of equation (4) captures the effect of active surveillance on eradication cost. The net effect depends on the relative magnitudes of the discount and spread rates. The discount rate reflects the rate at which a bank deposit increases over time. If the spread rate is larger, or equivalently, the eradication expenditure grows at a rate larger than the rate at which a bank deposit increases, a higher active surveillance budget will unambiguously reduce eradication costs. On the other hand, if the spread rate is smaller, early detection and eradication may increase the (present value) of the eradication cost.

It is also worth noting that a large discount rate and a small spread rate are not sufficient conditions for abandoning efforts to facilitate early detection and eradication, because a cumulatively growing loss that occurs when the threat spreads must also be considered (Kompas et al., 2016). If we denote d and F as the annual rate of loss caused by one invaded unit and the fixed component of the loss which does not vary with infection size, then the (expected) loss caused by the threat (summed over all entries and discounted to a present value) is:

$$
\begin{aligned}
L &= E\left\{\sum_{i=1}^{\infty}\left\{F\times e^{-\rho b_i}+d\int_{b_i}^{t(x_i)}x_i\left(t\right)e^{-\rho t}dt\right\}\right\}\\
&= \sum_{i=1}^{\infty}\left\{E\left\{e^{-\rho b_i}\right\}\times\left[F+d\times\int_{\widetilde{x}}^{\infty}\int_{0}^{t(x_i)-b_i}x_i\left(t\right)e^{-\rho t}dt\frac{\partial p\left(x_i,s\right)}{\partial x_i}dx_i\right]\right\} \qquad (5)\\
&= \frac{E\left\{e^{-\rho\varepsilon_i}\right\}\times e^{-\rho\Phi(q)}}{1-E\left\{e^{-\rho\varepsilon_i}\right\}\times e^{-\rho\Phi(q)}}\left[F+d\times\int_{\widetilde{x}}^{\infty}\int_{0}^{t(x_i)-b_i}x_i\left(t\right)e^{-\rho t}dt\frac{\partial p\left(x_i,s\right)}{\partial x_i}dx_i\right]
\end{aligned}
$$

We will use the expected eradication cost in equation (4) and the expected loss in equation (5) to determine the expenditures on prevention and active surveillance that minimise the total cost of the biosecurity measure itself, plus the expected eradication cost and losses associated with the invasive, or:

$$
\begin{aligned}
&\min_{\langle s\geq 0,q\geq 0\rangle}\sum_{n=1}\left\{L+B_e+B_q+B_s\right\}\\
&\text{subject to (4)–(5) and}\sum_{n=1}\left\{q+s\right\}\leq B
\end{aligned}
\qquad (6)
$$

where B is the annual total budget allocated to prevention and active surveillance of PFF, and B_q and B_s are the present value of the expenditures on prevention and active surveillance associated with annual budgets for prevention q and active surveillance s, respectively.

5.2 Functional forms

Optimization problems like (6) do not have analytical solutions, so we must rely on numerical techniques to solve the problem. To calibrate the model numerically, we specify that the drift of incursion time (i.e., the expected incursion interval) is a linear function of prevention expenditure and any uncertainty in incursion times follows a normal distribution, with a variance proportional to the expected incursion interval:

$$\begin{aligned} \Phi(q) &= \alpha + \beta q \\ D &\equiv N(0, \mu\Phi(q)) \end{aligned} \tag{7}$$

where α is the average interval between two entries without prevention, β measures the effectiveness of intervention and μ is the proportion of the variance of incursion time to the average incursion interval.

We also assume that the detection probability function takes the functional form:

$$\begin{aligned} p(x_i, s) &= \begin{cases} \frac{x_i}{\overline{x}(s)} \text{ if } x_i \in (0, \overline{x}(s)] \\ 1 \text{ if } x_i > \overline{x}(s) \end{cases} \\ \text{with } \overline{x}(s) &\equiv \left(\overline{X} - \widetilde{x}\right) e^{-\eta s} + \widetilde{x} \end{aligned} \tag{8}$$

where $\overline{X}$ is the passive-surveillance detection point (the point where the pest or disease has become so wide-spread that it will be recognised even without surveillance by experts, $\overline{x}(s)$ is the detection point with a given active surveillance effort s (the targeted detection point); and $\eta > 0$ is a parameter measuring active surveillance effectiveness.

Given the functional forms in equations (8) and (9), the expected eradication expenditure in equation (4), and the expected damage caused by the disease in equation (5) can be simplified as:

$$B_e = \frac{e^{-\rho(\alpha+\beta q)\left(1-\frac{\rho\mu}{2}\right)}}{1 - e^{-\rho(\alpha+\beta q)\left(1-\frac{\rho\mu}{2}\right)}} \times \frac{C(\widetilde{x})^{\frac{\rho}{r}}}{\left(2 - \frac{\rho}{r}\right)\overline{x}(s)} \times \left[\overline{x}(s)^{2-\frac{\rho}{r}} - (\widetilde{x})^{2-\frac{\rho}{r}}\right] \tag{9}$$

$$\begin{aligned} L = \frac{e^{-\rho(\alpha+\beta q)\left(1-\frac{\rho\mu}{2}\right)}}{1 - e^{-\rho(\alpha+\beta q)\left(1-\frac{\rho\mu}{2}\right)}} \times \Bigg\{ F + \frac{\widetilde{x} d}{\overline{x}(s)(r-\rho)} \times \\ \left[(\widetilde{x})^{\frac{\rho-r}{r}} \frac{r}{2r-\rho} \left(\overline{x}(s)^{\frac{2r-\rho}{r}} - (\widetilde{x})^{\frac{2r-\rho}{r}} \right) - (\overline{x}(s) - \widetilde{x}) \right] \Bigg\} \end{aligned} \tag{10}$$

5.3 Results

To illustrate the model, we first calibrate with a set of baseline parameters and vary these parameters to examine the sensitivity of the results. For the baseline scenario, we specify an annual discount rate of 3%, an approximation of the 'real interest rate' in Australia (i.e., the nominal interest rate minus the rate of inflation). The incursion probability, without border quarantine, is assumed to be 50% (i.e., on average one incursion every two years), and reduced to 5% (i.e., on average once every 20 years) if \$0.5 million dollars are spent on quarantine. The spread rate is calibrated under the assumption that PFF, if not eradicated, can spread from one to 1000 properties within a year. The natural detection size and the surveillance effectiveness are calibrated under the assumption that passive surveillance alone can detect PFF with 100%

certainty after four months, and spending $1m on active surveillance can reduce this detection time by 4 times (i.e., detection after one month). The initial pest incursion (if any) is for a farm which has an average value of $412,000 where the pest can reduce the value of affected properties by 45%. The eradication cost is calibrated assuming that, if not controlled, PFF causes an average cost of $1.567 billion a year. The calibration of the baseline parameters is summarised in Table 1 and largely draws on the estimates contained in CEBRA Project 1405C, *Baseline 'Consequence Measures' for Australia from the Torres Strait Islands Pathway to Queensland: Papaya Fruit Fly, Citrus Canker and Rabies.*

Table 1: Baseline parameter values for PFF

Parameter symbols	Parameters	Assumptions to calibrate
ρ	Discount rate	Annual discount rate is 3%, an approximation of nominal interest rate minus inflation in Australia.
α	Average incursion interval	Incursion probability without quarantine is 50% (on average, once every 2 years)
β	Quarantine effectiveness	On average, spending extra $0.5-million (on top of the existing level) for searching for possible PFF entry can reduce the incursion probability by 10 times, i.e., to 5% or on average, once every 20 years.
μ	Interval coefficient	The variance of the uncertainty in the incursion time is 100% of the incursion interval.
r	Spread rate	PFF in a farm can spread to 1000 properties in one year if not eradicated.
F	Fixed loss	There is no fixed loss associated with PFF.
C	Eradication cost	PFF can cause $1.567 billion a year in damages in the absence of quarantine and surveillance.
$\overline{X}$	Passive-surveillance detection point	Awareness enhancement programs could help detect the pest if it has spread to at least 10 farms.
η	Surveillance effectiveness	Spending $1 million on active surveillance (including traps, search, etc.) can reduce the detection time by 4 times (i.e., the pest will be detected after one month).
$\widetilde{x}$	Initial incursion	Initial incursion is 1 farm. The value of infected farm(s) is reduced by 45%.

Using these baseline parameter values, we calculate optimal quarantine and surveillance spending. The results are summarised in Figure 2. The figure shows that optimal quarantine and surveillance spending are $0.486 and $2.57 million a year for the study area, or put differently, the total spending is $3.056 million and the share between quarantine and surveillance is 16:84, or roughly 1:5. This optimal spending is relatively higher than the current budget for the Torres Strait Fruit Fly Strategy at $400K (Hafi et al., 2013, p19). With the optimal spending level, the incursion probability will be nearly 0.05, or in other words, once every 20 years, on average. It follows that at this optimal level of spending and detection, the total cost is nearly $3.468 million, and the sum of eradication expenditure and production loss is $0.412 million a year. This ($0.412 million) is an annualised value since eradication and production losses will only arise when incursions occur. This value reflects the amount that should be 'banked' every year

Figure 2: Baseline parameters

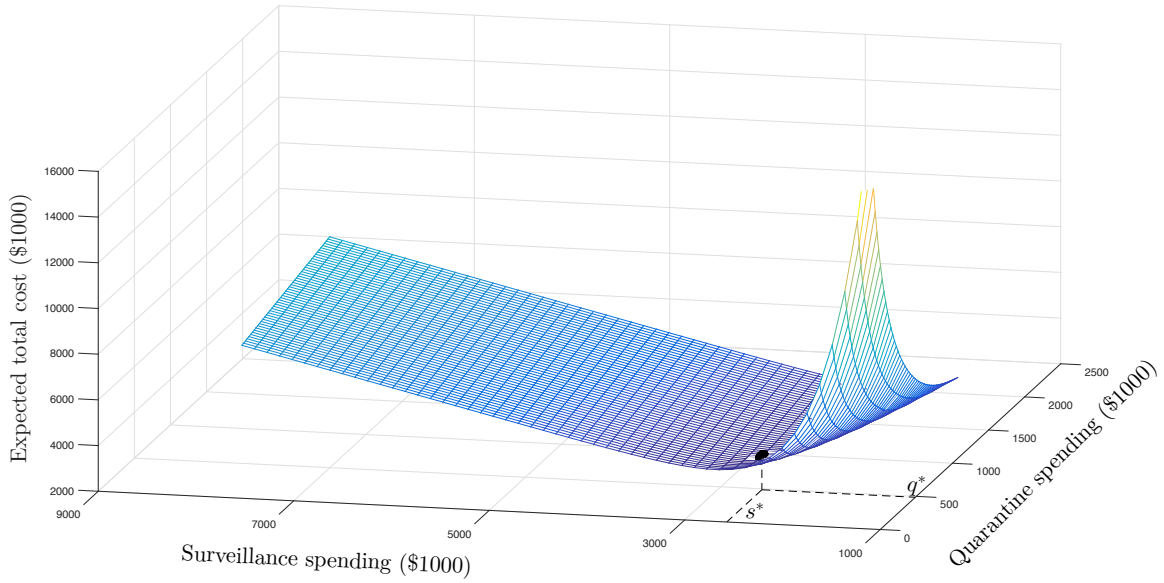

to spend on controlling PFF should an incursion take place. On average, each dollar spent on quarantine helps reduce the loss by $10 dollars, and each dollar spent on surveillance reduces the loss by $47.44 dollars.

To control for the possible uncertainty in the chosen baseline scenario, we examine how the optimal results vary with different parameter values. To do this, we vary some parameters while leaving all others unchanged and (repeatedly) solve for optimal quarantine and surveillance spending. This is referred to as a sensitivity analysis and, for brevity, we provide the results for key parameters in Tables 2-4 below. Sensitivity results for any other combinations of parameters can be undertaken upon request.

Table 2 shows the sensitivity for the incursion probability without quarantine together with quarantine effectiveness. For example, the first cells in two partitions imply that if the pest incursion occurs every year (incursion probability =1) and spending $0.5 million on quarantine can reduce the incursion probability by five times (i.e., from 1 to 0.2, or put in terms of frequency, from every year to once every five years), then total spending is $3.77 million of which 7% goes to quarantine and the remaining 93% goes to surveillance (or equivalently, $0.26 million for quarantine and $3.51 million for surveillance). The incursion probability decreases from top to bottom, and quarantine effectiveness increases from left to right. Moving from top to bottom, the table shows that as entries are less frequent, total spending declines. Also, as the probability of a pest incursion falls, so does the incentive for post-border control, and consequently the share of surveillance in total spending declines. Moving horizontally, as quarantine becomes more effective, total spending decreases and so does the share of surveillance in total spending since surveillance itself is relatively less effective. Given the modest choice for the baseline scenario of an incursion every two years without quarantine and that actual incursions could be more frequent, the two first rows of Table 2 (where $\alpha = 0.7$ and $\alpha = 1$) are more likely than the two last rows.

Table 2: Sensitivity analysis of incursion probability and quarantine effectiveness versus total spending on quarantine and surveillance ($m) and their shares (quarantine : surveillance)

Incursion probability without quarantine	Total spending ($m)					Shares in the total spending (quarantine : surveillance)				
	a $0.5-m quarantine program reduces incursion by X times					a $0.5-m quarantine program reduces incursion by X times				
	5	7	10	13	15	5	7	10	13	15
1	3.77	3.62	3.45	3.32	3.24	7:93	9:91	11:89	13:87	14:86
0.7	3.57	3.42	3.25	3.11	3.03	8:92	11:89	13:87	16:84	17:83
0.5	3.39	3.24	3.06	2.9	2.8	10:90	12:88	16:84	20:80	24:76
0.3	3.11	2.94	2.69	2.19	1.94	13:87	17:83	29:71	100:0	100:0
0.1	1.87	1.41	1.04	0.83	0.74	100:0	100:0	100:0	100:0	100:0

Table 3 shows the sensitivity for the detection time of passive surveillance and the effectiveness of active surveillance. The first cells of the two partitions imply that if passive surveillance can detect a PFF incursion after 15 farms are affected, and spending $1 million dollars on active surveillance reduces this by 50% or twice (so the active surveillance can detect after three months), then total spending will be $4.31 million, and the share between quarantine and (active) surveillance is 100:0. The effectiveness of passive surveillance increases from top to bottom, and the effectiveness of active surveillance increases from left to right. The results show that when passive surveillance is more effective, total spending declines. Also, as the pest can be detected early after incursion, there is less need for border quarantine so that the share of quarantine measures in total spending declines. Moving horizontally, spending and the share for quarantine both decline as active surveillance is becomes relatively more effective.

Table 3: Sensitivity analysis of the effectiveness of passive and active surveillance versus total spending on quarantine and surveillance ($m) and their shares (quarantine : surveillance)

Passive surveillance can detect when X farms become affected	Total spending ($m)					Shares in the total spending (quarantine : surveillance)				
	A $1-m surveillance program reduces detection time by Y times					A $1-m surveillance program reduces detection time by Y times				
	2	3	4	5	6	2	3	4	5	6
15	4.31	3.81	3.37	3.11	2.92	100:0	23:77	18:82	17:83	15:85
13	4.29	3.63	3.22	2.97	2.8	84:16	20:80	17:83	15:85	15:85
10	4.26	3.45	3.06	2.83	2.67	34:66	19:81	16:84	15:85	14:86
7	4.12	3.31	2.94	2.72	2.57	29:71	18:82	15:85	14:86	13:87
5	4.04	3.24	2.88	2.67	2.53	28:72	17:83	15:85	14:86	13:87

Table 4 shows sensitivity for the loss rate of infected properties and the spread rate of PFF. The first cells of the two partitions imply that if each affected farm loses 35% of its value, and PFF can spread from 1 to 500 properties within a year if not controlled, then the total spending

is $2.95 million, and the share between border quarantine and surveillance expenditures is 18:82. Total spending slightly increases with the loss rate (top to bottom) as the pest cause more damage, but remain unchanged (roughly with two-digit rounding) in the chosen range of spread rates (left to right). Moving in both directions, the post-border biosecurity threat becomes more significant and the share of expenditures on surveillance increases.

Table 4: Sensitivity analysis of loss rates and spread rates

Loss rate of infected properties	Total spending ($m)					Shares in the total spending (quarantine : surveillance)				
	How many properties PFF can spread in a year (if not treated)					How many properties PFF can spread in a year (if not treated)				
	500	750	1000	1250	1500	500	750	1000	1250	1500
35%	2.95	2.95	2.95	2.95	2.95	18:82	17:83	17:83	16:84	16:84
40%	3	3.01	3.01	3.01	3.01	18:82	17:83	16:84	16:84	15:85
45%	3.06	3.06	3.06	3.06	3.06	17:83	16:84	16:84	16:84	15:85
50%	3.1	3.1	3.1	3.1	3.1	17:83	16:84	16:84	15:85	15:85
55%	3.14	3.14	3.14	3.14	3.14	17:83	16:84	15:85	15:85	15:85

6 PFF Surveillance from a Spatial Perspective

In this section, given various border biosecurity measures, and thus arrival/establishment rates, our goal is to find the optimal level of spending on local traps to detect PFF early, considering its potential benefit in reducing the economic damages of a potential PFF outbreak. To do so, we develop a random dispersal model to characterise the movement of PFF while incorporating time, spatial heterogeneity, seasonal features and randomness. We then overlay an economic model on top of this random dispersal model to form a stochastic spatial dynamic programming surveillance problem.

6.1 Random dispersal model

Consider a land area divided into q small raster cells which is either habitable (i.e., is a suitable host) or non-habitable (i.e., is not a suitable host) to PFF. The cell is small enough that the within-cell PFF population growth can be ignored. At the outset, a PFF group 'settles' in a random habitable cell from an outside source. As the PFF population grows, part of the population will form 'departing propagules' and migrate in various directions in search for new habitable cells or hosts, thus potentially threatening an otherwise substantial horticultural industry.

We divide the PFF life cycle into two stages. The early development stage lasts for four weeks when PFF develop from egg to larva and then pupa. During this stage, they stay 'latent' at the host (Yonow et al., 2004). In the adult stage, which lasts for another ten weeks, PFF can potentially reproduce, and more importantly migrate to other hosts and spread the outbreak (Yonow et al., 2004). We assume adult PFF migrate as propagules to ensure their successful reproduction in a new host, and we set the time step in our model as weekly so as it is in line with the PFF life cycle.

Propagule dispersal is characterised by three important factors, namely range, direction and the quantity of released propagules (Adeva et al., 2012). In terms of range, some PFF can make a jump over a long distance r_{jump} in the first week of their adult stage when they are the strongest and most active (Adeva et al., 2012; Dominiak, 2012). We denote α as the probability of a propagule to make such a jump. The propagules that do not make a long jump stay in the neighbourhood and move locally within a range r_{local} per week. Depending on whether a propagule moves locally or over a long distance, the actual distance it makes is a random event following uniform distributions unif$(0, r_{\text{local}})$ or unif$(0, r_{\text{jump}})$, respectively. With regard to direction, a propagule making a long jump does so in any directions. After the long jump, it travels in a similar way as the ones that stay local. The movement direction of locally-travelling propagules depends on the proximity of a nearby host since PFF can sense its presence (Adeva et al., 2012). We denote the probability of PFF to find a nearby host as $\beta(d)$ – a function of d, the distance from a propagule to a host. When $\beta(d)$ is equal to zero, that is, all hosts are too far away for PFF to detect, they will move randomly in any direction. Finally, the number of propagules released from each host per week, π, depends on seasonal features such as wind, temperature, soil moisture, and host suitability, etc. (Bateman, 1967; Yonow et al., 2004; Dominiak et al., 2003). Thus, with randomness in range, direction and quantity of released propagules fully considered, our dispersal model is basically random in nature.

The dispersal process in our model can be represented in an extended network as shown in Figure 3. In panel (a), solid circles represent hosts or cells that are habitable for PFF while the broken ones are not. Starting from host C, propagules are released to find new hosts, expanding their colony. They can find a new host within one period of time (e.g., propagule f_2^C), or they can land on a non-habitable cell and have to keep searching until they find a new host (e.g., propagule f_1^C). If a host has already been occupied, an arriving propagule has to leave immediately and continue their search for a new host in the next period (e.g. propagule f_3^C). The reason is that eggs are inserted directly into the host fruit and once larvae starts to feed, an unidentified change occurs in the fruit, which generally causes females to avoid it (Waterhouse and Sands, 2001). Our dispersal model can be perceived easier in panel (b), where all non-habitable nodes and 'unsuccessful' connections (i.e., connections to/from non-habitable cells) are hidden, and therefore, a node at a particular time step t can contact multiple nodes at the following time steps within the length of a PFF adult stage.

For easy presentation and computation, we identify all habitable cells (X) in the research area while suppressing all inhabitable ones. We denote x_{it} as the infestation state of a habitable cell i at time t where x_{it} can take either of the two values: x_{it}=1 means the cell is infested while x_{it}=0 means the cell is susceptible. We denote $\boldsymbol{X_t}$ as a vector of infestation states of all habitable cells at time t. At $t = 0$, there is only one cell infested. An infected cell can release new flies every time period and the flies can live for some period of time, disperse from the original cell and affect other habitable cells along their journey. Therefore, moving forward in time, the infestation state of each cell i at time t where $t > 0$, depends on four factors: (i) all the cells' infestation states in the previous A time periods [$\boldsymbol{X_{t-1}}$, ..., $\boldsymbol{X_{t-A}}$] where A is the length of the PFF adult stage or the life span of a PFF propagule, during which it can survive and search for a new host to colonise; (ii) the realisation of the above mentioned random factors to the dispersed propagules in the dispersal model over the last A time periods, jointly denoted as vectors $\boldsymbol{\xi_{t-A}}, \dddot{,} \boldsymbol{\xi_{t-1}}$, where the dimension of $\boldsymbol{\xi_t}$ is the total number of released propagules; (iii) the realisation of the probability of an infested cell getting detected without using traps during the last A time periods $\gamma_{t-A}, \dddot{,} \gamma_{t-1}$, where the dimension of γ_t is the total number of traps; and (iv) the grid size of traps g (i.e., the larger the grid is, the fewer traps are required). As a result, the random dispersal of PFF over time and heterogenous space can be expressed

as:

$$X_t = f(\boldsymbol{X_{t-1}, ..., X_{t-A}}; \boldsymbol{\xi_{t-1}, ..., \xi_{t-A}}; \gamma_{t-1}, ..., \gamma_{t-A}; g) = f(\boldsymbol{\Xi_t}; X_0; g) \tag{11}$$

where, for short notation, $\boldsymbol{\Xi_{t-1}}$ is a matrix combining all information on the realisations of random events before t; and X_0 is the initial condition, i.e., the cell where an outbreak starts.

Figure 3: Papaya Fruit Fly random network dispersal model

(a) With non-habitable nodes

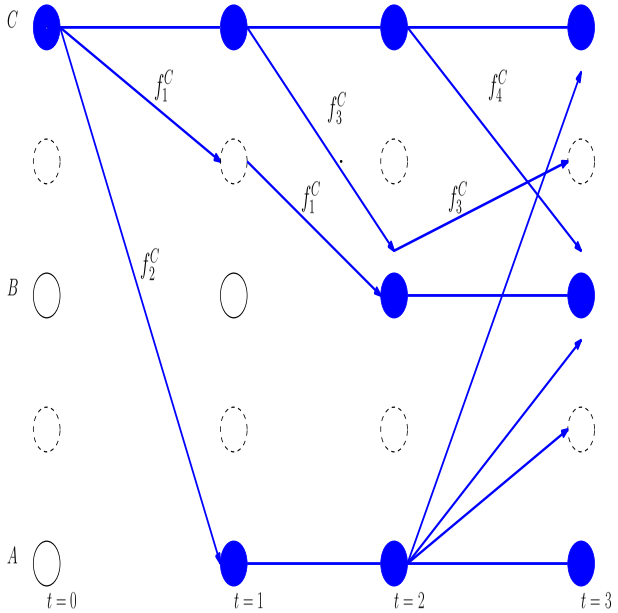

(b) Without non-habitable nodes

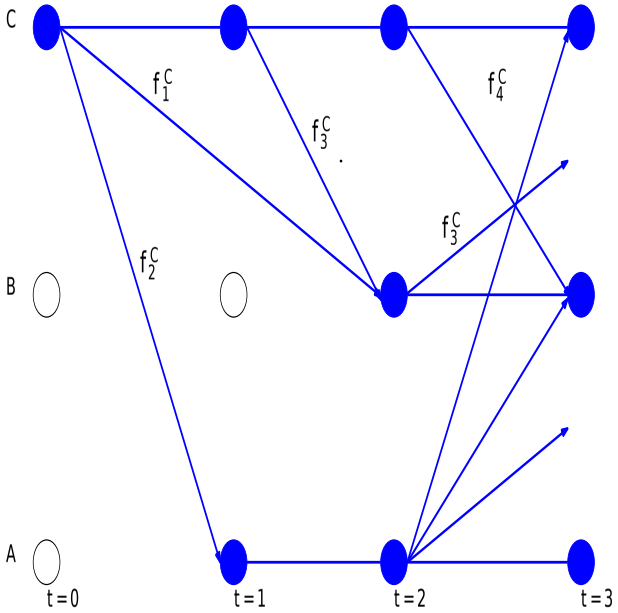

6.2 Economic model

Without any interventions, an infested cell will eventually be detected by farmers, typically by visual inspection of fruit (Cantrell et al., 2002). This point of detection might be termed a 'natural detection point' indicating a detection made without the aid of any surveillance measures such as traps. Currently, local traps are the only surveillance measure to detect PFF early so that an outbreak, if it happens, would be small (Cantrell et al., 2002; Kompas and Che, 2009). The question is whether it is worthwhile to lay local traps and how much to spend on them (i.e., how dense should the trapping network be) so that the total cost of controlling a PFF outbreak, along with total damages and the cost of detecting it early, is the smallest.

To find the optimal level of local traps, we specify all cost components. They include: (i) a PFF outbreak control cost, (ii) suspension cost; (iii) production losses, (iv) revenue losses due to trade sanctions and loss of market access, and (v) surveillance cost or the cost of detecting PFF early. It is worth mentioning that the surveillance cost is an on-going cost while the first three cost items are incurred largely after PFF is detected. For simplicity, we ignore production losses incurred before a PFF detection since they would be very small.

Outbreak control costs incur once PFF is detected at a host. Then control/eradication activities will be carried out at the host and the eradication zone surrounding it on a radius of $r_{\text{eradication}}$, where infested hosts and propagules will be treated and terminated. Similar to the approach in Epanchin-Niell et al. (2012b), the expected control cost of an outbreak, C^E, is:

$$C^E(g) = \lambda \times \mathbb{E}D'_{\mathcal{T}}(\boldsymbol{\Xi}_{\boldsymbol{\mathcal{T}}}; X_0; g) \times c^{\text{e}} \tag{12}$$

where λ is the outbreak arrival rate (probability); $\mathcal{T}$ is an outbreak duration; $D_{\mathcal{T}}$ is an indication vector of dimension X representing whether a habitable cell has PFF detected or not and/or whether it belongs to an eradication zone formed during an outbreak. For simplicity, we apply eradication to a cell only once within an outbreak, and c^{e} is a control cost for each raster cell. It is worth noting that we use a different time notation τ to reflect the point that the summation in Equation 18 is over an outbreak duration. Moreover, the expected control cost of an outbreak is product of the average of outbreak control costs and the outbreak arrival rate since we can get an outbreak every year with a probability of λ. Finally, given all the randomness and exogenous parameters, C^E is a function of grid size g.

Suspension cost is the additional cost of spraying the fruit before it can be sold from suspension area C^Z. Similar to the above eradication cost, suspension cost can be defined as follows:

$$C^Z(g) = \lambda \times \mathbb{E}\sum_{t}^{\mathcal{T}} Z'_t(\boldsymbol{\Xi}_{\boldsymbol{t-1}}; X_0; g) \times c^{\text{T}} \tag{13}$$

where Z_t is an indication vector of dimension X representing whether a habitable cell has PFF detected or not and/or whether it belongs to an suspension zone at t; and c^{T} is a vector of weekly suspension costs for habitable raster cells. c^{T} depends on the cost of fruit management (spraying) and production volume, hence it will be cell-specific.

Likewise, the expected production loss due to PFF eradication activities is:

$$C^P(g) = \lambda \times \mathbb{E}\sum_{t}^{\mathcal{T}} P'_t(\boldsymbol{\Xi}_{\boldsymbol{t-1}}; X_0; g) \times \boldsymbol{c^p V^p} \tag{14}$$

where P_t is an indication vector dimension X representing whether a habitable cell is in the eradication zone at t; $\boldsymbol{c^p}$ and $\boldsymbol{V^p}$ are $X \times 1$ vectors of production loss and weekly production values, being specific for each individual raster cell, and T^{m} is the management time for each detection.

In the same fashion, at every time t, with a probability λ of a new outbreak, we have a λ chance of getting a trade sanction and loss of market access. Accordingly, this trade sanction and loss of market access costs the following expected revenues losses, C^R:

$$C^R(g) = \lambda \times \mathbb{E}[T^{\text{outbreak}}(\boldsymbol{\Xi}_{\boldsymbol{\mathcal{T}}}; X_0; g) + T^{\text{mkt}}] \times c^{\text{r}} \tag{15}$$

where $T^{\text{outbreak}}(\boldsymbol{\Xi}_{\boldsymbol{\tau}}; X_0; \beta; g)$ is the outbreak duration or time between first and last detection while T^{mkt} is the waiting time to gain back full market access; and c^r is the weekly trade related revenue loss.

Finally, following Florec et al. (2010), the on-going surveillance cost, C^S, is:

$$C^S(g) = Q \times \left(\frac{w_I + \delta w_S + E}{X} + c^q\right) \tag{16}$$

where Q is the number of traps; w_I and w_S are weekly inspector and supervisor wages, respectively, while δ is the ratio of a supervisor to inspectors; E is the weekly equipment cost; c^q is the weekly cost of maintaining a trap; and X is the number of traps inspected per week, calculated as:

$$X = \frac{h}{\left(\frac{l}{v}\right) + m} \tag{17}$$

where h is the weekly working hours per each inspector/supervisor, l is the travel distance between traps, v is the speed of travelling between traps, and m is the time spent on checking each trap. The 'pest quarantine area' (PQA) management cost is

$$C^M(g) = \lambda \times \mathbb{E}M_{\mathcal{T}}(\boldsymbol{\Xi}_{\boldsymbol{\mathcal{T}}}; X_0; g) \times c^{\text{m}} \tag{18}$$

where $M_{\mathcal{T}}$ is an indication vector dimension X representing whether a habitable cell is in the PQA during the outbreak; and c^{m} is value of management cost assigned to each cell.

To sum up, our surveillance optimization problem is of the form:

$$\min_g TC = \min_g(C^E + C^Z + C^P + C^M + C^R + C^S) \equiv \min_g \mathbb{E}[f(\boldsymbol{\Xi}, g)] \tag{19}$$

By design, the idea is to minimise all of the losses associated with a potential PFF incursion and spread and the cost of the surveillance program itself. The more dense is the trapping grid, the more expensive is the surveillance activity, but detection is also earlier and potential damages smaller. On the other hand, the less dense is the trapping grid, the smaller are surveillance expenditures but potential damages from an incursion and spread are much larger and the probability of eradication is less.

6.3 Planning horizon

In terms of planning horizon, we choose an initial fixed period of 15 months for our optimisation problem. Any outbreak that is (estimated to be) longer than 15 months will be treated as a severe outbreak and will ignite a national eradication campaign. The 15 month period is similar to the time it took from the first incursion until the massive eradication campaign was initiated in Queensland in 1995. Before the eradication campaign, any positive detection (by traps) will incur a 15 km eradication and suspension zone around the detection point (Dominiak, 2007). If that eradication measure fails to eradicate the flies at the end of the 15 months period, a national eradication campaign will be kicked off. In that case, a massive rectangular PQA would ensue, which includes an 80 km buffer zone around infected cells, similar to the area defined in the 1995 outbreak (see Figure 4a). Road blocks and additional traps will be established

in this area to enforce movement (fruits) restriction and to determine the outbreak size. We assume the PQA management cost will be proportional to the outbreak size (the number of cells in PQA areas). This cost is approximately 13.5 million Cantrell et al. (2002) in total and is divided by the 1995 outbreak size to determine per cell management costs. In addition to the PQA, once a national eradication campaign has been kicked off, all (existing) suspension zones will be extended to include the 80 km buffer zone around detection points. All fruits from suspension zones must be treated (sprays and disinfestation), with inspectors' audit and approval. These additional measures in the national eradication campaign are designed to mimic the 1995 eradication campaign (see Cantrell et al., 2002).

Figure 4: PFF outbreak in north Queensland in Novermber 1995: actual versus simulated infestations

(a) Actual infestations

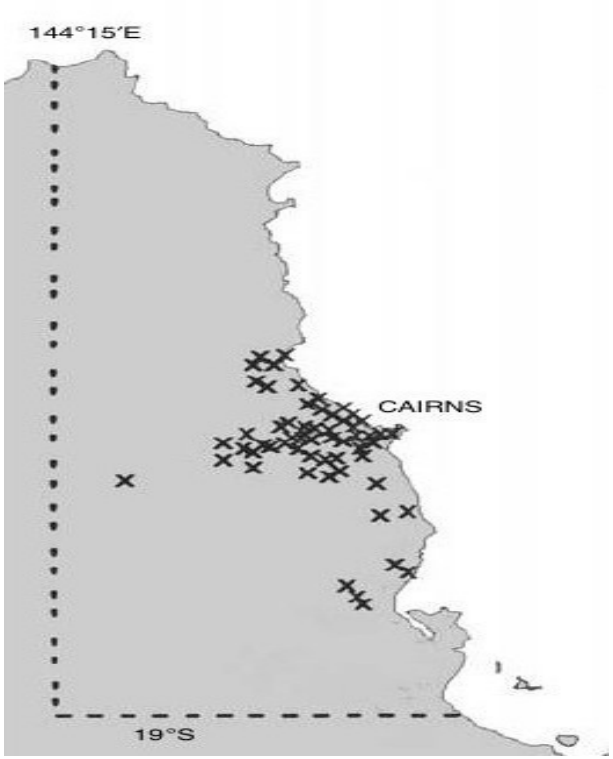

Source: Fay et al. (1997, p.260b)

(b) Simulated infestations

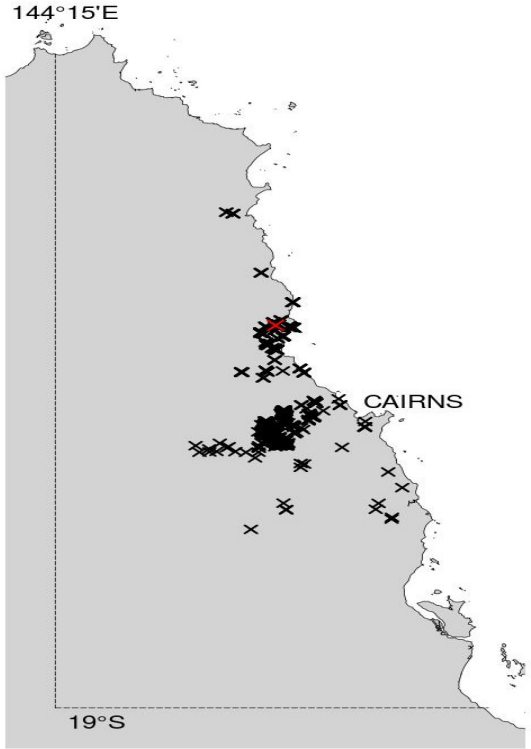

Source: Authors' calculation.

6.4 Sample Average Approximation

We use a SAA method to solve the optimisation problem in equation (19) since the usual dynamic programming method cannot be applied due to the curse of dimensionality (Bellman, 2003). SAA can handle this large dimension while yielding consistent solution estimates due to the use of a combination of exterior sampling and deterministic optimisation methods (Norkin et al., 1998; Mak et al., 1999; Shapiro, 2003). The idea is to generate samples of $\{\mathbf{\Xi_1}, \mathbf{\Xi_2}, \ldots, \mathbf{\Xi_Z}\}$, and then the 'true' solution to the problem in equation (19) is approximated by sample averages in conjunction with direct search methods. The exterior sampling method makes the problem simpler and able to be solved more efficiently because the random matrix $\mathbf{\Xi}$ is realised outside the optimisation routine (Shapiro, 2003).

With regard to implementation, SAA involves a three-stage procedure, being repeated until convergence towards the true objective function value TC^* is achieved. In the first stage, a lower bound for TC^* is estimated as:

$$\overline{TC}_{N,M} = \frac{1}{M} \sum_{m=1}^{M} \overline{TC}_N^m \tag{20}$$

where $\overline{TC}_N^1, \overline{TC}_N^2, \ldots, \overline{TC}_N^M$ are minimum values obtained from M independently and identically distributed (iid) generated samples of size N:

$$\overline{TC}_N^m = \min_g \frac{1}{N} \sum_{n=1}^{N} TC(\Xi_n^m, g) \tag{21}$$

Associated with these objective values are candidate policy solutions $\hat{g}^1, \hat{g}^2, \ldots, \hat{g}^M$. In the second stage, an iid sample of size N', typically being much larger than N will be generated to identify the best solution among $\hat{g}^m$. The best candidate solution $\hat{g}^*$ selected is the one that gives the smallest objective value, or:

$$\hat{g}^* \in \arg\min\{\frac{1}{N'} \sum_{n'=1}^{N'} TC(\Xi_{n'}, \hat{g}) : \hat{g} \in \{\hat{g}^1, \hat{g}^2, \ldots, \hat{g}^M\}\} \tag{22}$$

In the third stage, to obtain an unbiased estimate (Verweij et al., 2003; Sheldon et al., 2010; Ahmadizadeh et al., 2010), another iid sample N'', being also much larger than N, is generated independently from previous samples to estimate an upper bound for TC^* by:

$$\widehat{TC}_{N''}(\hat{g}^*) = \frac{1}{N''} \sum_{n''=1}^{N''} TC(\hat{g}^*, \Xi_{n''}) \tag{23}$$

The 'optimality gap' is estimated as:

$$\mathbf{gap}(\hat{g}^*) = \widehat{TC}_{N''}(\hat{g}^*) - \overline{TC}_{N,M} \tag{24}$$

The smaller the $\mathbf{gap}(\hat{g}^*)$ the better the quality of the solution. The three-stage procedure repeats with increasing sample sizes, especially for N, until the $\mathbf{gap}(\hat{g}^*)$ is small enough to ensure convergence of the estimated solution to the true solution.

With SAA being based on Monte Carlo simulation techniques, estimators in equations (20–24) are random. They can be shown to be consistent using some regularity conditions from the

'Law of Large Numbers' (LLN). The spreads of their sampling distributions or the variances are estimated as:

$$\begin{aligned}
\hat{\sigma}^2_{\overline{TC}_{N,M}} &= \frac{1}{(M-1)M}\sum_{m=1}^{M}\left(TC_N^m - \overline{TC}_{N,M}\right)^2 \\
\hat{\sigma}^2_{\widehat{TC}_{N''}(\hat{g}^*)} &= \frac{1}{(N''-1)N''}\sum_{n''=1}^{N''}\left(TC(\hat{g}^*,\Xi_{n''}) - \widehat{TC}_{N''}(\hat{g}^*)\right)^2 \\
\hat{\sigma}^2_{\mathbf{gap}(\hat{g}^*)} &= \hat{\sigma}^2_{\widehat{TC}_{N''}(\hat{g}^*)} + \hat{\sigma}^2_{\overline{TC}_{N,M}}
\end{aligned} \tag{25}$$

6.5 Parallel processing

Detailed spatial heterogeneity coupled with the need to keep track of all propagules results in an incredibly large-sized problem which cannot be addressed efficiently by serial computing. Therefore, following Kompas et al. (2015), we use a parallel processing algorithm which employs several computers and processes at the same time to solve the problem more efficiently. In particular, we apply parallel processing to both simulation and optimisation. We use several processes, in other words, in several computers to simultaneously generate many fractions of sample size N, N' and N'', and calculate sample averages as specified in equations (20) and (23) across processes by sending their outputs to a master process. Similar to an optimisation process which is based on direct search for the optimal point, we also use several computers and processes to simultaneously calculate equation (22) which applies various policies to a large samples N' and N''. In like manner, equation (24) can be executed in parallel. In short, a combination of SAA and parallel processing makes this incredibly large-sized problem possible to be solved.

7 Results

In this section, we describe all parameter values used in our model. We then present model results, followed by a sensitivity analysis. Numerical results and plots are obtained using *C* and *R* programming software.

7.1 Parameterisation

The outbreak in our model starts from an invasion by PFF migrating from Papua New Guinea via the Torres Strait islands. This event is by far the most likely PFF threat for Queensland. The Torres Strait Fruit Fly Strategy has been designed to prevent permanent establishment of exotic fruit flies in the Torres Strait to reduce the risk of them moving south to mainland Australia, via Queensland (Plant Health Committee, 2013). Given this prior, we limit the PFF incursion in Queensland to an area of about 1000 raster cells in the far north of Queensland (above 16.5^{o}S latitude), which are close to the Torres Strait Islands and more likely to be invaded first. A PFF outbreak begins when flies settle in a random cell within the incursion area. Once settled, PFF will gradually expand in a southerly direction.

All of the parameter values used in our model are presented in Table 5. The research area as shown in Figure 1 is 1.85 million km^2 in area, which is divided into approximately 1.4 billion $50m \times 50m$ raster cells. A detailed land use raster map of this area, from ABARES (2015), provides us with information on six broad categories of land use, with up to as many as 60 different smaller land use purposes in each category. Based on this map and the fact that PFF

infest only horticultural areas, we classify the research area into about 1.4 billion non-habitable and about 0.53 million habitable raster cells.

Table 5: Model parameterisation

Pameter	Description	Unit	Value
	Random Dispersal Model		
λ	Outbreak arrival rate (probability)[(a)]	per week	0.2/52
A	Life span of a PFF propagule[(b)]	week	10
α	Probability of a PFF propagule to make a long jump[(c)]		0.3
r_{jump}	Maximum distance of a long jump[(d)]	km/1^{st} week	94
r_{local}	Maximum distance of local travel[(c)]	km/week	1.4
β	Probability of a PFF to find a nearby host[(c)]		Equation 26
π	Number of propagules released from each infested cell[(e)]	#/per week	2
	Economic Model		
$r_{\text{eradication}}$	Radius for eradication zone[(d)]	km	15
c^{e}	One-off control cost[(a)]	\$/per km^2	539
c^{r}	Weekly trade-related revenue loss[(f)]	\$ mil/week	25/52
c^{m}	PQA management cost[(k)]	\$/per cell	114
T^{mkt}	Length of international market closure[(g)]	month	8.5
T^{m}	Management time after each detection[(h)]	month	8.5
γ	Probability of an infested cell getting detected without using traps[(h)]		[0,1]
c^{p}	Production loss[(i)]	percent	45
h	Number of working hours per week[(j)]	hour	37
v	Speed of travelling between traps	km/h	40
m	Time spent at each trap[(j)]	minute	4.14
c^{q}	Cost of trap maintenance[(j)]	\$/week	9.75/52
E	Equipment cost (cars)[(j)]	per week	15,000/52
δ	Ratio of supervisor to inspectors [(j)]		1/3
w_I	Inspector's salary[(j)]	\$/week	66,700/52
w_S	Supervisor's salary[(j)]	\$/week	82,200/52

Notes: All values will be converted Australian Dollar 2015. [(a)]Kompas and Che (2009); [(b)]Bateman (1967), Yonow et al. (2004) & Adeva et al. (2012); [(c)]Adeva et al. (2012); [(d)]Dominiak (2007); [(e)]Authors' calibration based on actual infestation Fay et al. (1997, p.260b) & Atlas of Living Australia (2015). [(f)]Cantrell et al. (2002); [(g)]Underwood (2007); [(h)]Authors' assumption; [(i)]Authors' estimation based on Queensland's horticulture gross production revenue, in particular, Fruit: \$864.77 million, Vegetables and herbs: \$376.66 million, Citrus:\$ 83.18 million, Grapes: \$55.67 million (Australian Bureau of Statistics, 2011); [(j)]Florec et al. (2010).[(k)] Authors' calculation from Cantrell et al. (2002).

Parameter values for the random dispersal model are largely drawn from the literature. In particular, the outbreak arrival rate is one in every five years (Kompas and Che, 2009). The length of a PFF adult stage or life span of a propagule is 10 weeks, during which it can survive and search for a new host to colonise (Bateman, 1967; Yonow et al., 2004; Adeva et al., 2012). The probability of a propagule to make a long jump is 0.3 based on the dispersal distribution in Adeva et al. (2012) while the maximum distance of local travel and a long jump are 1.4 km/week and 94km/week, respectively (Adeva et al., 2012; Dominiak, 2012).

Adopted from Adeva et al. (2012, p. 101), the probability of PFF to find a nearby host is defined as follows:

$$\beta(d) = \begin{cases} -0.0513d^3 + 0.335d^2 - 0.904d + 1.083 & \text{if } d \leq 3 \text{ km} \\ 0 & \text{if } d > 3 \text{ km} \end{cases} \tag{26}$$

where d is the distance from a propagule to a host. Equation (26) ensures that a propagule will detect a habitable host within 0.1 km with certainty. Additionally, the further away a habitable host is, the less certain a propagule can detect it. When habitable hosts are located beyond 3km away, a propagule cannot detect it, thereby having to keep moving randomly in direction until it finds a habitable host to colonise, or die due to lack of food or reaching the end of their life. In line with equation (26), we assume that a PFF will be detected with certainty if within 500m around a trap which uses baits to attract PFF in the same way as a host does.

A key parameter in the random dispersal model is the number of propagules released from each infested cell. This parameter is important since it largely determines the extent of PFF spread, hence the size of a PFF outbreak. We calibrate this parameter value based on two sources of information. The first one is the historical information on the spread of the first PFF outbreak in north Queensland in 1995. It is widely believed that PFF were present for 12-15 months before the massive eradication campaign in October of that year (Cantrell et al., 2002). Therefore, in our simulations, we let PFF disperse freely (undetected) for 16 months (4 weeks silent) using our random dispersal model, and compare our simulated infestations with the actual ones in Queensland in November 1995. Panel (b) in Figure 4 shows infested raster cells in a medium-sized outbreak among our simulation runs. With two propagules released from an infested cell per week on average, our model can replicate well the actual infestations during the same period as shown in panel (a). Note that panel (b) only depicts infested cells, not travelling propagules. With travelling propagules taken into account, we expect a larger outbreak, and hence our simulated results would look even more similar to the actual outbreak. The second source of information is the monthly occurrence records of fruit flies (*Bactrocera (Bactrocera) tryoni*) in Queensland from 1950s (Atlas of Living Australia, 2015). Since PFF and Bactrocera (Bactrocera) tryoni belong to the same genus, Bactrocera, they share some common biological characteristics including seasonal patterns of incursion and migration. For this reason, we can use information on Bactrocera (Bactrocera) tryoni as a proxy to estimate seasonal patterns of PFF. These estimated seasonal patterns are then incorporated into our calibration of the number of propagules released per week (see Table 6).

Table 6: Seasonal factor for fruit fly incursion in Queensland.

Month	Jan	Feb	Mar	Apr	May	Jun	Jul	Aug	Sep	Oct	Nov	Dec
Seasonal factor	1.75	0.608	2.20	0.987	0.911	0.0759	0.228	1.97	0.456	0.911	0.532	1.37

Source: Authors' calculation from Atlas of Living Australia (2015).

Parameter values for the economic model are also largely drawn from the literature. In particular, the radius for the eradication zone surrounding an infested and detected host is 15 km, following Dominiak (2012). The one-off control cost for each raster cell is calculated based on the rate of \$539 per km^2, largely to cover labour and chemicals as used in a previous study by Kompas and Che (2009). Weekly trade-related revenue loss is estimated based on the corresponding \$100 million loss to producers incurred in the first PFF outbreak in Queensland in 1995 (Cantrell et al., 2002). We choose this estimate in spite of the availability of more updated estimates for the whole of Australia (e.g. Hafi et al., 2013) since it comes from an actual outbreak and the outbreak occurred in our study area. The length of international market closure T^{mkt} is 8.5 months following Underwood (2007).

Production losses, clearly, are raster-cell-specific. This complicates matters. We combine land use information with data on production value by crop and local areas from Australian Bureau of Statistics (2011) to calculate the production value for each cell. While some raster cells are categorised as specific to citrus and grape growing areas, the majority of cells can only

be designated by 'general horticultural use', given by perennial, seasonal, irrigated perennial, irrigated seasonal, and intensive horticulture. Therefore, for each specific horticultural use, we approximate annual production value for a cell by dividing the corresponding horticultural production value across the appropriate cells. For the remainder of the other uses, we use their production value shares to adjust their cell values. Finally, we assume the production loss is 45% of the cell production value. This is half of the maximum damage rate used in Kompas and Che (2009), reflecting the loss due to flies and limited access to domestic markets, while the duration of this loss or the management time after each detection in a cell and its surrounding eradication area is assumed to be 8.5 months, or the same time length as the international market closure (Kiwifruit Vine Health, 2014).

In terms of on-going surveillance cost we use estimates of cost components from Florec et al. (2010). Since we don't know the exact travel distance between traps, we assume that it is the same as the grid size (or as the 'crow flies distance') between traps. This assumption slightly underestimates surveillance costs.

Finally, the probability of a cell getting detected without using traps is assumed to be zero if the cell is infested for less than six months, and to be one otherwise. The reason for this is that PFF is hard to detect. Its eggs are inserted directly into the host fruit well before it ripens, and the rapidly growing tissues quickly cover any marks made by the fruit fly, making it difficult for all but the trained eye to see where eggs had been laid (Cantrell et al., 2002). Since PFF makes infested fruit look ripe earlier, this attracts the attention of growers and causes notice, and thus is eventually detected. Therefore, we assume that it takes six months for an infestation to be naturally detected as this is the average time it would take horticultural crops in Queensland, such as bananas, to ripen.

7.2 SAA Numerical Results

To get numerical results for Equation 19, parallel processing was carried out using 12 processes over 3 quad core CPU computers with Hyper-Threading. This parallel processing implementation helps increase the possible simulation numbers in our computing system by 12 fold, compared to a similar uni-processing process. As shown in Table 7, when repeating the three-stage procedure of SAA specified in equations (8–11), we increase the sample size N until the optimal gaps are stabilised at less than 1% ($N \to 672$), while keeping M, the number of samples, constant at 50. As a result, the number of simulations in the first stage increases by up to 33,600 simulations. In the second and third stages, the sample sizes N' and N'' used to find the candidate optimal solution and check its quality remain constant at 33,600. Algorithms used for our computation are available upon request.

Numerical results are presented in Figure 5. As can be seen, there is a trade-off between spending on early detection and the cost of an outbreak. In particular, we find that the optimal grid size of local traps, $\hat{g}^*$, is around 0.7 km, which is equivalent to about 6,782 traps to be laid (See Table 7 when $\lambda = .2$). With this level of traps, the minimised total expected outbreak cost is approximately \$7.7 million and the annual on-going surveillance cost is approximately \$2.08 million.

We also pay attention to the outbreak arrival rate as it is directly related to pre-border and border quarantine controls. Table 7 shows the optimal surveillance grid size at different arrival rates. The Table indicates that an increase in the outbreak arrival rate λ increases the optimum number of traps (or equivalently reduces grid size). The optimum grid size (distance between traps) increases to 750 m when λ is less than 15%. The grid size, however, remains unchanged from its optimum point of 700m when λ increases to 15% and beyond. In our particular value range of λ (from 0.05 to 0.5), the optimum grid size is rigid against λ. The benefit of early

detection depends on how much benefit we gain when we have an early detection system in place or how fast the outbreak grows undetected. This depends on the biological characteristic of the species and the environment. The arrival rate will not change that, rather it relates more to the trade-off between the cost of surveillance system and the benefit of early detection.

Figure 5: Total expected outbreak cost of PFF surveillance.

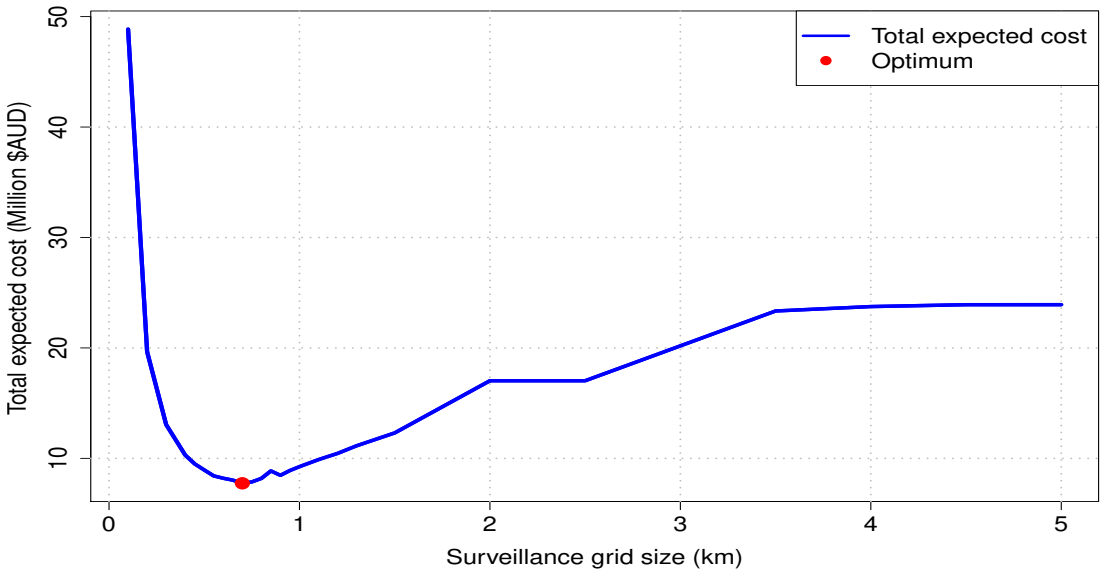

We next compare our results with the current grid size for traps in Queensland. As shown in Figure 6, the traps currently laid are less dense than that in the optimal case. Indeed, the grid size of traps in Queensland is 5km (Kompas and Che, 2009) compared to the optimal grid size level of 0.7 km suggested in our paper. While this density of traps implies a much lower surveillance cost per year, $92.9 thousand versus $2.08 million under the optimal policy, the expected total outbreak cost under the current scenario is $23.92 million which is much higher than the optimal case (Figure 5).

Figure 6: Local traps laid: current versus optimal

(a) Current Policy

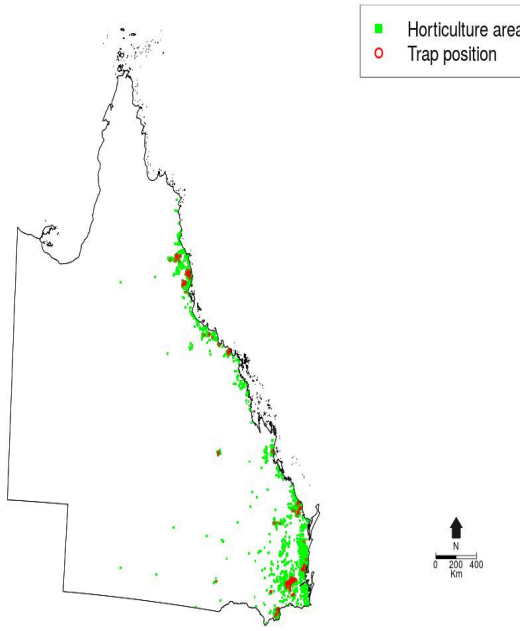

(b) Optimal Policy

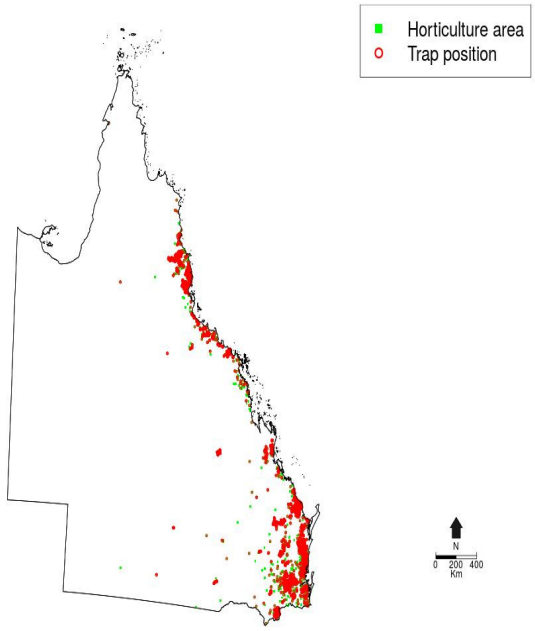

Table 7: Estimated expected PFF outbreak costs and optimality gaps at different arrival rates

N	48	144	240	336	432	528	576	624	672
Arrival rate $\lambda = 0.05$									
Optimal trap grid size (km)	0.75	0.75	0.75	0.75	0.75	0.75	0.75	0.75	0.75
Lower bound (A)	4.738	4.794	4.813	4.826	4.821	4.839	4.833	4.834	4.831
	(0.025)	(0.015)	(0.011)	(0.011)	(0.009)	(0.009)	(0.008)	(0.007)	(0.008)
Upper bound (B)	4.832	4.827	4.829	4.839	4.843	4.841	4.831	4.834	4.835
	(0.007)	(0.007)	(0.007)	(0.007)	(0.007)	(0.008)	(0.007)	(0.007)	(0.007)
Optimality gap (C=B - A)	0.094	0.034	0.016	0.014	0.021	0.003	-0.002	0.000	0.004
	(0.033)	(0.022)	(0.018)	(0.019)	(0.016)	(0.016)	(0.015)	(0.015)	(0.016)
Percentage of the lower bound D=(C/A)*100%	1.985	0.701	0.326	0.283	0.444	0.059	-0.046	0.001	0.076
Arrival rate $\lambda = 0.10$									
Optimal trap grid size (km)	0.75	0.75	0.75	0.75	0.75	0.75	0.75	0.75	0.75
Lower bound (A)	4.738	4.794	4.813	4.826	4.821	4.839	4.833	4.834	4.831
	(0.025)	(0.015)	(0.011)	(0.011)	(0.009)	(0.009)	(0.008)	(0.007)	(0.008)
Upper bound (B)	4.832	4.827	4.829	4.839	4.843	4.841	4.831	4.834	4.835
	(0.007)	(0.007)	(0.007)	(0.007)	(0.007)	(0.008)	(0.007)	(0.007)	(0.007)
Optimality gap (C=B - A)	0.094	0.034	0.016	0.014	0.021	0.003	-0.002	0.000	0.004
	(0.033)	(0.022)	(0.018)	(0.019)	(0.016)	(0.016)	(0.015)	(0.015)	(0.016)
Percentage of the lower bound D=(C/A)*100%	1.985	0.701	0.326	0.283	0.444	0.059	-0.046	0.001	0.076
Arrival rate $\lambda = 0.15$									
Optimal trap grid size (km)	0.7	0.7	0.7	0.7	0.7	0.7	0.7	0.7	0.7
Lower bound (A)	6.214	6.280	6.295	6.307	6.303	6.318	6.321	6.317	6.316
	(0.023)	(0.014)	(0.010)	(0.009)	(0.008)	(0.007)	(0.008)	(0.006)	(0.005)
Upper bound (B)	6.332	6.332	6.324	6.326	6.332	6.328	6.330	6.330	6.327
	(0.005)	(0.005)	(0.005)	(0.005)	(0.005)	(0.005)	(0.005)	(0.005)	(0.005)
Optimality gap (C=B - A)	0.117	0.051	0.029	0.019	0.029	0.010	0.009	0.013	0.011
	(0.028)	(0.018)	(0.015)	(0.014)	(0.012)	(0.012)	(0.013)	(0.011)	(0.010)
Percentage of the lower bound D=(C/A)*100%	1.888	0.815	0.464	0.306	0.453	0.158	0.145	0.212	0.173
Arrival rate $\lambda = 0.20$									
Optimal trap grid size (km)	0.7	0.7	0.7	0.7	0.7	0.7	0.7	0.7	0.7
Lower bound (A)	7.656	7.714	7.730	7.743	7.735	7.745	7.755	7.744	7.736
	(0.024)	(0.015)	(0.011)	(0.009)	(0.007)	(0.007)	(0.009)	(0.009)	(0.006)

Table 7 – continued from previous page

N	48	144	240	336	432	528	576	624	672
Upper bound (B)	7.749	7.749	7.739	7.742	7.749	7.744	7.746	7.747	7.742
	(0.007)	(0.007)	(0.006)	(0.006)	(0.006)	(0.006)	(0.006)	(0.007)	(0.006)
Optimality gap (C=B - A)	0.093	0.035	0.009	-0.002	0.013	-0.001	-0.009	0.003	0.006
	(0.031)	(0.021)	(0.017)	(0.016)	(0.014)	(0.013)	(0.015)	(0.015)	(0.012)
Percentage of the lower bound D=(C/A)*100%	1.216	0.449	0.123	-0.019	0.174	-0.014	-0.112	0.045	0.078
Arrival rate $\lambda = 0.25$									
Optimal trap grid size (km)	0.7	0.7	0.7	0.7	0.7	0.7	0.7	0.7	0.7
Lower bound (A)	9.075	9.133	9.155	9.164	9.157	9.166	9.174	9.161	9.150
	(0.027)	(0.017)	(0.013)	(0.011)	(0.009)	(0.008)	(0.011)	(0.010)	(0.007)
Upper bound (B)	9.166	9.166	9.154	9.157	9.166	9.160	9.163	9.164	9.158
	(0.008)	(0.008)	(0.008)	(0.008)	(0.008)	(0.008)	(0.008)	(0.008)	(0.008)
Optimality gap (C=B - A)	0.091	0.033	-0.001	-0.007	0.009	-0.006	-0.011	0.003	0.008
	(0.035)	(0.025)	(0.021)	(0.019)	(0.017)	(0.016)	(0.019)	(0.019)	(0.015)
Percentage of the lower bound D=(C/A)*100%	1.007	0.357	-0.014	-0.072	0.100	-0.064	-0.118	0.030	0.083
Arrival rate $\lambda = 0.30$									
Optimal trap grid size (km)	0.7	0.7	0.7	0.7	0.7	0.7	0.7	0.7	0.7
Lower bound (A)	10.489	10.550	10.571	10.583	10.573	10.584	10.592	10.578	10.565
	(0.030)	(0.019)	(0.015)	(0.013)	(0.010)	(0.009)	(0.013)	(0.012)	(0.009)
Upper bound (B)	10.584	10.583	10.568	10.572	10.583	10.576	10.579	10.581	10.574
	(0.010)	(0.010)	(0.009)	(0.009)	(0.009)	(0.009)	(0.010)	(0.010)	(0.009)
Optimality gap (C=B - A)	0.094	0.033	-0.003	-0.010	0.009	-0.009	-0.013	0.003	0.009
	(0.040)	(0.029)	(0.024)	(0.022)	(0.020)	(0.019)	(0.023)	(0.022)	(0.018)
Percentage of the lower bound D=(C/A)*100%	0.898	0.310	-0.024	-0.098	0.090	-0.081	-0.123	0.030	0.086
Arrival rate $\lambda = 0.35$									
Optimal trap grid size (km)	0.7	0.7	0.7	0.7	0.7	0.7	0.7	0.7	0.7
Lower bound (A)	11.901	11.966	11.985	12.002	11.989	12.002	12.011	11.994	11.979
	(0.033)	(0.022)	(0.017)	(0.014)	(0.012)	(0.011)	(0.015)	(0.015)	(0.010)
Upper bound (B)	12.001	12.000	11.983	11.988	12.000	11.992	11.996	11.998	11.989
	(0.011)	(0.011)	(0.011)	(0.011)	(0.011)	(0.011)	(0.011)	(0.011)	(0.011)
Optimality gap (C=B - A)	0.100	0.035	-0.002	-0.014	0.011	-0.010	-0.015	0.004	0.011
	(0.045)	(0.033)	(0.028)	(0.026)	(0.023)	(0.022)	(0.027)	(0.026)	(0.021)
Percentage of the lower bound	0.837	0.288	-0.019	-0.117	0.089	-0.086	-0.126	0.031	0.089

Table 7 – continued from previous page

N	48	144	240	336	432	528	576	624	672
D=(C/A)*100%									
Arrival rate $\lambda = 0.40$									
Optimal trap grid size (km)	0.7	0.7	0.7	0.7	0.7	0.7	0.7	0.7	0.7
Lower bound (A)	13.311	13.379	13.399	13.421	13.405	13.420	13.430	13.410	13.393
	(0.036)	(0.025)	(0.019)	(0.016)	(0.014)	(0.012)	(0.018)	(0.017)	(0.012)
Upper bound (B)	13.418	13.417	13.398	13.403	13.417	13.408	13.412	13.414	13.405
	(0.013)	(0.013)	(0.012)	(0.013)	(0.013)	(0.013)	(0.013)	(0.013)	(0.012)
Optimality gap (C=B - A)	0.107	0.038	-0.001	-0.018	0.012	-0.012	-0.017	0.004	0.012
	(0.049)	(0.038)	(0.031)	(0.029)	(0.026)	(0.025)	(0.030)	(0.030)	(0.024)
Percentage of the lower bound D=(C/A)*100%	0.806	0.282	-0.006	-0.133	0.091	-0.088	-0.129	0.031	0.091
Arrival rate $\lambda = 0.45$									
Optimal trap grid size (km)	0.7	0.7	0.7	0.7	0.7	0.7	0.7	0.7	0.7
Lower bound (A)	14.719	14.793	14.812	14.840	14.821	14.837	14.848	14.826	14.807
	(0.040)	(0.028)	(0.021)	(0.018)	(0.015)	(0.014)	(0.020)	(0.019)	(0.013)
Upper bound (B)	14.835	14.834	14.813	14.819	14.834	14.824	14.829	14.831	14.820
	(0.015)	(0.015)	(0.014)	(0.014)	(0.014)	(0.014)	(0.014)	(0.015)	(0.014)
Optimality gap (C=B - A)	0.116	0.042	0.001	-0.021	0.014	-0.013	-0.020	0.005	0.014
	(0.054)	(0.042)	(0.035)	(0.033)	(0.029)	(0.028)	(0.034)	(0.033)	(0.027)
Percentage of the lower bound D=(C/A)*100%	0.789	0.281	0.004	-0.145	0.093	-0.090	-0.131	0.032	0.092
Arrival rate $\lambda = 0.50$									
Optimal trap grid size (km)	0.7	0.7	0.7	0.7	0.7	0.7	0.7	0.7	0.7
Lower bound (A)	16.124	16.204	16.225	16.258	16.236	16.254	16.267	16.243	16.221
	(0.042)	(0.030)	(0.023)	(0.020)	(0.017)	(0.016)	(0.022)	(0.021)	(0.015)
Upper bound (B)	16.253	16.251	16.227	16.234	16.251	16.240	16.246	16.248	16.236
	(0.016)	(0.016)	(0.015)	(0.016)	(0.016)	(0.016)	(0.016)	(0.016)	(0.015)
Optimality gap (C=B - A)	0.128	0.047	0.002	-0.024	0.015	-0.015	-0.022	0.005	0.015
	(0.059)	(0.046)	(0.038)	(0.036)	(0.033)	(0.031)	(0.038)	(0.037)	(0.030)
Percentage of the lower bound D=(C/A)*100%	0.794	0.290	0.012	-0.149	0.094	-0.091	-0.133	0.032	0.094

M = 50; $N' = N$"=33,600; Number of processes = 12. Values in AUD Million (2014). Standard errors in parentheses. All estimates are significant at 1% level except for the ones of the optimal gap which are statistically insignificant at any conventional levels.

Finally, our results support previous studies applied in a similar context (Kompas and Che, 2009; White et al., 2012). (Kompas and Che, 2009) suggested a 60% increase in surveillance expenses in Australia, which mean a denser surveillance grid. Meanwhile, (White et al., 2012) also suggest an optimal grid of 700 and 1000 m over the Sunraysia region across northern Victoria and western New South Wales, Australia.

7.3 Sensitivity Analysis

In this subsection, we check whether our results are sensitive to key parameter values. It is important to note that unlike deterministic models, our model fully incorporates randomness, and the SAA optimisation itself method relies on LLN to ensure our solution estimate converges to its true solution (i.e., is consistent) as the sample size or the number of simulations increases. Changes in parameter values will alter the data generating process for simulations. New solution estimates, therefore, reflect the changes in parameter values, not randomness. We aim to compare these new estimates with our main result to see how sensitive the results are due to changes in parameter values.

We focus on the key parameters of the random dispersal model and the economic model. They include the number of propagules released from each infested cell, trade sanction duration, PQA management cost, production loss, and travel distance between traps. These parameters are hard to estimate precisely but are instrumental in determining the extent of an outbreak. Other parameters have a relatively minor impact on model results, and are not discussed here for brevity. Detailed results are available upon request.

The optimum surveillance grid size is sensitive to the number of propagules released from each infested cell. Figure 7a shows that an increase in the number of propagules released from each infested cell will imply an increase in the distance between traps and thus reduce the number of traps. More propagules released make flies easier to detect.

On the other hand, the economic model parameters have less influence on the optimum grid size. In our baseline scenario, we assume 8.5 months trade sanctions after the last positive detection. This assumption is inline with suspension time in the suspension area. The trade sanction, however, could be longer than that. In Figure 7b we try to measure the impact of ± 20 change in trade sanction duration to our optimal surveillance problem. The Figure shows that the change in trade sanction duration does affect the expected total cost of a PFF invasion, but not the optimum surveillance grid itself.

The production loss factor $\boldsymbol{c^p}$ also has little impact on the optimum surveillance grid. We choose $\boldsymbol{c^p}$ as half of the maximum damage rate in (Kompas and Che, 2009). The rate may vary in practice for different invasions. Figure 7c shows the robustness of our result in such a situation.

The third economic model parameter we need to look at is the PQA management cost parameter c^{m}. We assume the management cost is proportional to the size of the PQA (number of habitable cells in PQA). Since these are a fixed component of management costs, c^{m} could vary from invasion to invasion. Fortunately, Figure 7d shows little impact from changes in c^{m} to optimal grid size. In fact, the impact of c^{m} is insignificant when the grid size is close to an optimum point (or lower), because the PQA is less likely to be initiated in stricter surveillance regimes.

The last, but perhaps most important, economic model parameter is the travel distance between traps l in Equation 17. Following Florec et al. (2010) we proxy this distance by trap grid size. The travel distance, in fact, will vary considerably in practice, especially with a coarser grid and a highly spatial and heterogeneous area. In order to access the diversity of l, we calculate the mean distance between traps in each row from left to right and from the

last cell of a row to the beginning cell of the next cell. This serves as an estimation of a upper bound of l because the long distances in this calculation will generally not be realised. Figure 7e shows how the change in l from our baseline case to that upper bound would affect our optimum surveillance measures. From the Figure, it is clear that l will significantly impact expected total cost. The impact is strongest around the optimum point. This is not a surprise, although l is expected to be much larger than grid size in coarser grids. The number of traps reduces exponentially with coarser grids and this outweighs the change in l. Similarly with denser grids, the number of traps increases exponentially while l approaches the grid size. The optimal surveillance grid is, however, relatively unchanged with the change in l.

8 Conclusion

PFF is a clear and proven danger to Australia horticulture industry. A long term strategy is in place for controlling fruit flies in the Torres Strait to prevent them from invading mainland Australia. However, the Torres Strait surveillance activity cannot prevent every possible incursion, and traps are still routinely used on the mainland of Australia to further protect against a possible incursion. In this paper, we do two things. First, we construct and calibrate a basic model for the allocation of resources between border and post-border measures. Second, we design a spatial stochastic dynamic model to study the movement of PFF in Queensland and to predict the outcomes of potential PFF incursions. We also design an early detection surveillance grid accounting for both a temporal dimension and heterogeneous space.

Using a new optimisation technique, in a novel way, we solve for an optimal surveillance program determining the best grid size to detect PFF early. Our method captures far more detail than the aggregate approach to these problems and is more efficient than simulation approaches at finding an optimal outcome. The results indicate a grid size of less than 1 km, suggesting that not enough resources for biosecurity are being directed to this activity in Queensland. Border and post-border expenditures occur in at a 1:4 ratio given our parameter set.

Figure 7: Sensitivity Analysis

(a) Number of propagules released each week

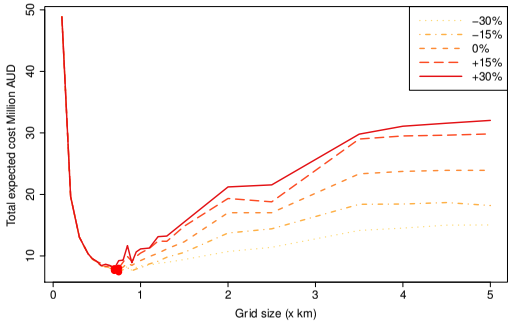

(b) Trade sanction duration

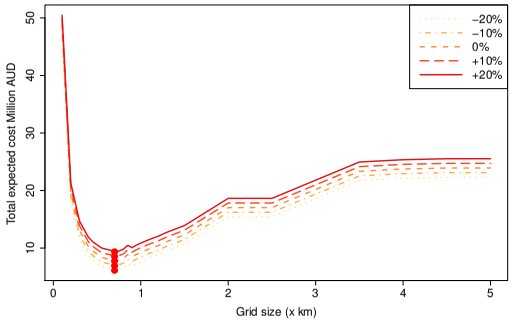

(c) Production loss factor

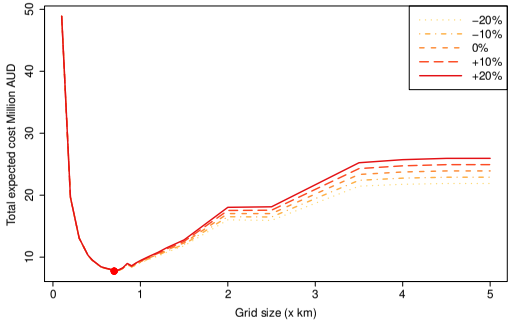

(d) Pest Quarantine Area management cost

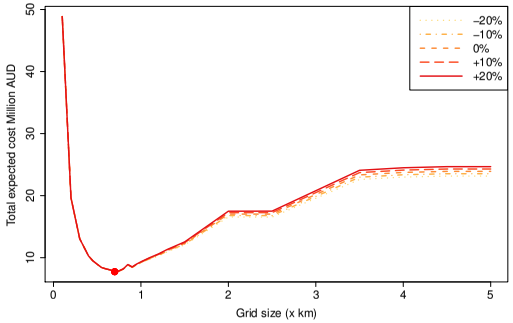

(e) Grid factors (% of the gap).

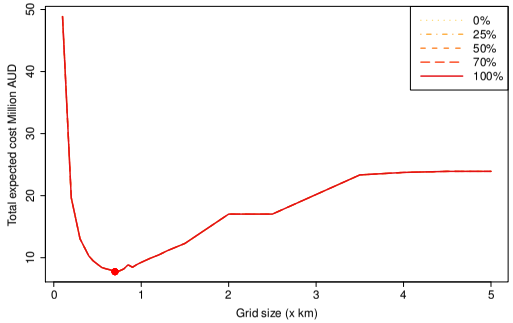

References

ABARES, 2015. Catchment scale land use of Australia - Update March 2015. Available at http://data.daff.gov.au/anrdl/metadata_files/pb_luausg9abll20150415_11a.xml [Accessed: 25 June 2015].

Adeva, J. G., Botha, J., Reynolds, M., 2012. A simulation modelling approach to forecast establishment and spread of bactrocera fruit flies. Ecological Modelling 227 (0), 93 – 108.

Ahmadizadeh, K., Dilkina, B., Gomes, C. P., Sabharwal, A., 2010. An empirical study of optimization for maximizing diffusion in networks. In: Cohen, D. (Ed.), Principles and Practice of Constraint Programming – CP 2010: 16th International Conference, CP 2010, St. Andrews, Scotland, September 6-10, 2010. Proceedings. Springer Berlin Heidelberg, Berlin, Heidelberg, pp. 514–521.

Akter, S., Kompas, T., Ward, M. B., 2015. Application of portfolio theory to asset-based biosecurity decision analysis. Ecological Economics 117, 73–85.

Albers, H. J., Fischer, C., Sanchirico, J. N., 2010. Invasive species management in a spatially heterogeneous world: Effects of uniform policies. Resource and Energy Economics 32 (4), 483–499.

Allwood, A. J., Drew, R. A. I., et al. (Eds.), 1997. Management of fruit flies in the Pacific. A regional symposium, Nadi, Fiji 28-31 October 1996. ACIAR proceedings.

Atallah, S. S., Gómez, M. I., Conrad, J. M., Nyrop, J. P., 2014. A plant-level, spatial, bioeconomic model of plant disease diffusion and control: Grapevine leafroll disease. American Journal of Agricultural Economics 97, 199–218.

Atlas of Living Australia, 2015. Bactrocera (bactrocera) tryoni. Available at websiteat:http://biocache.ala.org.au/occurrences/search?q=Bactrocera+(Bactrocera)+tryoni [Accessed: 25 June 2015].

Australian Bureau of Statistics, 2011. Agricultural commodities, Australia, 2010-2011. Available at http://www.abs.gov.au/AUSSTATS/abs@.nsf/Lookup/7121.0Main+Features12010-11 [Accessed: 21 January 2014].

Barnes, B., 2016. Sterile insect technique (SIT) for fruit fly control-the South African experience.
URL https://www.scopus.com/inward/record.uri?eid=2-s2.0-85028838125&doi=10.1007%2f978-3-319-43226-7_19&partnerID=40&md5=0f092f7b5d965a764a4d4af9f818b9a4

Bateman, M., Jan. 1967. Adaptations to temperature in geographic races of the Queensland fruit fly Dacus (Strumenta) tryoni. Australian Journal of Zoology 15 (6), 1141–1161.

Bellman, R., 2003. Dynamic Programming. New York: Dover Publications, Inc.

Billah, M., Afreh-Nuamah, K., Obeng-Ofori, D., Nyarko, G., et al., 2015. Review of the pest status, economic impact and management of fruit-infesting flies (Diptera: Tephritidae) in Africa. African Journal of Agricultural Research 10 (12), 1488–1498.

Blackwood, J., Hastings, A., Costello, C., 2010. Cost-effective management of invasive species using linear-quadratic control. Ecological Economics 69 (3), 519–527.

Bogich, T. L., Liebhold, A. M., Shea, K., 2008. To sample or eradicate? a cost minimization model for monitoring and managing an invasive species. Journal of Applied Ecology 45 (4), 1134–1142.

Butchart, S. H., Walpole, M., Collen, B., van Strien, A., Scharlemann, J. P., Almond, R. E., Baillie, J. E., Bomhard, B., Brown, C., Bruno, J., et al., 2010. Global biodiversity: indicators of recent declines. Science 328 (5982), 1164–1168.

Cantrell, B., Chadwick, B., Cahill, A., 2002. Fruit fly fighters: eradication of the papaya fruit fly. CSIRO Publishing.

Clark, R. A., Weems Jr, H. V., 1988. Detection, quarantine, and eradication of fruit flies invading Florida. In: AliNiazee, M. T. (Ed.), Ecology and Management of Economically Important Fruit Flies. pp. 73–81.

DAFF, 2005. Papaya fruit fly. Available at `https://www.business.qld.gov.au/industry/agriculture/land-management/health-pests-weeds-diseases/weeds-and-diseases/surveillance-programs/papaya-fruit-fly` [Accessed: 26 June 2015].

Ding, W., Gross, L. J., Langston, K., Lenhart, S., Real, L. A., 2007. Rabies in raccoons: optimal control for a discrete time model on a spatial grid. Journal of Biological Dynamics 1 (4), 379–393.

Dominiak, B., 2007. Fruit fly eradication in the Fruit Fly Exclusion Zone: questions and answers. NSW DPI, Prime fact 552.

Dominiak, B. C., May 2012. Review of dispersal, survival, and establishment of Bactrocera tryoni (Diptera: Tephritidae) for quarantine purposes. Annals of the Entomological Society of America 105 (3), 434–446.

Dominiak, B. C., Westcott, A. E., Barchia, I. M., Jan. 2003. Release of sterile Queensland fruit fly, Bactrocera tryoni (Froggatt) (Diptera: Tephritidae), at Sydney, Australia. Australian Journal of Experimental Agriculture 43 (5), 519–528.

Epanchin-Niell, R. S., Haight, R. G., Berec, L., Kean, J. M., Liebhold, A. M., 2012a. Optimal surveillance and eradication of invasive species in heterogeneous landscapes. Ecology Letters 15 (8), 803–812.

Epanchin-Niell, R. S., Haight, R. G., Berec, L., Kean, J. M., Liebhold, A. M., 2012b. Optimal surveillance and eradication of invasive species in heterogeneous landscapes. Ecology Letters 15 (8), 803–812.

Epanchin-Niell, R. S., Wilen, J. E., Mar. 2012. Optimal spatial control of biological invasions. Journal of Environmental Economics and Management 63 (2), 260–270.

Fay, H., Drew, R., Lloyd, A., 1997. The eradication program for papaya fruit fly (Bactrocera papayae Drew and Hancock) in North Queensland. In: A.J., A., R.A.I., D. (Eds.), Management of fruit flies in the Pacific. 76. ACIAR Proceedings, pp. 259–261.

Ferguson, N. M., Donnelly, C. A., Anderson, R. M., 2001. The foot-and-mouth epidemic in great britain: pattern of spread and impact of interventions. Science 292 (5519), 1155–1160.

Finnoff, D., Potapov, A., Lewis, M. A., 2010a. Control and the management of a spreading invader. Resource and Energy Economics 32 (4), 534–550.

Finnoff, D., Potapov, A., Lewis, M. A., 2010b. Second best policies in invasive species management: when are they "good enough"? In: Perrings, C., Mooney, H., Williamson, M. (Eds.), Bioinvasions and globalisation: ecology, economics, management, and policy. Oxford University Press, pp. 110–126.

Florec, V., Sadler, R., White, B., Aug. 2010. Surveillance in Fruit Flies Free Areas: An Economic Analysis. Working Papers 100882, University of Western Australia, School of Agricultural and Resource Economics.

Florec, V., Sadler, R. J., White, B., Dominiak, B. C., 2013. Choosing the battles: The economics of area wide pest management for Queensland fruit fly. Food Policy 38, 203–213.

Gramig, B. M., Horan, R. D., 2011. Jointly determined livestock disease dynamics and decentralised economic behaviour. Australian Journal of Agricultural and Resource Economics 55 (3), 393–410.

Grube, A., Donaldson, D., Kiely, T., Wu, L., 2011. Pesticides industry sales and usage: 2006 and 2007 market estimates. Biological and Economic Analysis Division, Office of Pesticide Programs, Office of Chemical Safety and Pollution Prevention, U.S. Environmental Protection Agency, Washington, DC 20460.

Gurevitch, J., Padilla, D. K., 2004. Are invasive species a major cause of extinctions? Trends in Ecology and Evolution 19 (9), 470–474.

Hafi, A., Arthur, T., Symes, M., Millist, N., 2013. Benefit-cost analysis of the long term containment strategy for exotic fruit flies in the Torres Strait. Report to client prepared for the National Biosecurity Committee, Canberra.

Hagen, K., Allen, W., Tassan, R., et al., 1981. Mediterranean fruit fly: the worst may be yet to come. California Agriculture 35 (3), 5–7.

Hauser, C. E., McCarthy, M. A., 2009. Streamlining search and destroy: cost-effective surveillance for invasive species management. Ecology Letters 12 (7), 683–692.

Hayama, Y., Yamamoto, T., Kobayashi, S., Muroga, N., Tsutsui, T., 2013. Mathematical model of the 2010 foot-and-mouth disease epidemic in Japan and evaluation of control measures. Preventive Veterinary Medicine 112 (3), 183–193.

Horie, T., Haight, R. G., Homans, F. R., Venette, R. C., 2013. Optimal strategies for the surveillance and control of forest pathogens: A case study with oak wilt. Ecological Economics 86, 78–85.

Keeling, M. J., Woolhouse, M. E. J., May, R. M., Davies, G., Grenfell, B. T., Jan. 2003. Modelling vaccination strategies against foot-and-mouth disease. Nature 421 (6919), 136–142.

Keeling, M. J., Woolhouse, M. E. J., Shaw, D. J., Matthews, L., Chase-Topping, M., Haydon, D. T., Cornell, S. J., Kappey, J., Wilesmith, J., Grenfell, B. T., 2001. Dynamics of the 2001 UK foot and mouth epidemic: stochastic dispersal in a heterogeneous landscape. Science 294 (5543), 813–817.

Kiwifruit Vine Health, March 2014. Financial impact of a fruit fly incursion to New Zealand's kiwifruit industry. Available at `http://www.kvh.org.nz/vdb/document/98983` [Accessed: 26 July 2016].

Kobayashi, M., Carpenter, T. E., Dickey, B. F., Howitt, R. E., 2007. A dynamic, optimal disease control model for foot-and-mouth disease: I. Model description. Preventive Veterinary Medicine 79 (2), 257–273.

Kompas, T., Che, N., 2009. A practical optimal surveillance measure: the case of papaya fruit fly in Australia. Australian Centre for Biosecurity and Environmental Economics, ANU; Centre of Excellence for Biosecurity Risk Analysis, University of Melbourne.

Kompas, T., Chu, L., Nguyen, H. T. M., 2016. A practical optimal surveillance policy for invasive weeds: An application to Hawkweed in Australia. Ecological Economics 130, 156–165.

Kompas, T., Ha, P. V., Nguyen, H. T. M., East, I., Roche, S., Garner, G., forthcoming. Optimal surveillance against foot-and-mouth disease: the case of bulk milk testing in Australia. Australian Journal of Agricultural and Resource Economics.
URL `http://dx.doi.org/10.1111/1467-8489.12224`

Kompas, T., Ha, P. V., Nguyen, H. T. M., Garner, G., 2015. Optimal surveillance against Transboundary Animal Disease in Heterogeneous Spaces. Australian Centre for Biosecurity and Environmental Economics, Crawford School of Public Policy, Australian National University; Centre of Excellence for Biosecurity Risk Analysis, University of Melbourne.

Kot, M., Lewis, M. A., van den Driessche, P., 1996. Dispersal data and the spread of invading organisms. Ecology 77 (7), 2027–2042.

Mak, W.-K., Morton, D. P., Wood, R. K., 1999. Monte carlo bounding techniques for determining solution quality in stochastic programs. Operations Research Letters 24 (1), 47–56.

Meentemeyer, R. K., Haas, S. E., Václavík, T., 2012. Landscape epidemiology of emerging infectious diseases in natural and human-altered ecosystems. Annual Review of Phytopathology 50, 379–402.

Mehta, S. V., Haight, R. G., Homans, F. R., Polasky, S., Venette, R. C., 2007. Optimal detection and control strategies for invasive species management. Ecological Economics 61 (2), 237–245.

Morris, R. S., Stern, M. W., Stevenson, M. A., Wilesmith, J. W., Sanson, R. L., 2001. Predictive spatial modelling of alternative control strategies for the foot-and-mouth disease epidemic in Great Britain, 2001. Veterinary Record 149 (5), 137–144.

National Research Council, 1992. Restoration of aquatic ecosystems: science, technology, and public policy. National Academy Press: Washington DC.

NISC, 2001. Meeting the invasive species challenge: National invasive species management plan. National Invasive Species Council. Available at `http://www.invasivespeciesinfo.gov/docs/council/mpfinal.pdf` [Accessed: 21 June 2015].

NISC, 2008. 2008–2012 National Invasive Species Management Plan. Available at `www.invasivespecies.gov` [Accessed: 20 April 2015].

Norkin, V. I., Pflug, G. C., Ruszczyński, A., 1998. A branch and bound method for stochastic global optimization. Mathematical Programming 83 (1-3), 425–450.

Olson, L. J., et al., 2006. The economics of terrestrial invasive species: a review of the literature. Agricultural and Resource Economics Review 35 (1), 178.

Pierre, R. Y., 2007. Economic impact of a Mediterranean fruit fly outbreak in Florida. Ph.D. thesis, University of Florida.

Pimentel, D., Lach, L., Zuniga, R., Morrison, D., 2000. Environmental and economic costs of nonindigenous species in the United States. BioScience 50 (1), 53–65.

Plant Health Committee, 2013. Review of the long-term containment strategy for exotic fruit flies in Torres Strait. Available at `http://www.planthealthaustralia.com.au/national-programs/fruit-fly/` [Accessed: 20 August 2016].

Robinson, A., 2002. Genetic sexing strains in medfly, ceratitis capitata, sterile insect technique programmes. Genetica 116 (1), 5–13, cited By 53.
URL `https://www.scopus.com/inward/record.uri?eid=2-s2.0-0036760891&doi=10.1023%2fA%3a1020951407069&partnerID=40&md5=b6cbca5a950dd70206b8bcb8f4203d30`

Sanchirico, J. N., Albers, H. J., Fischer, C., Coleman, C., 2010. Spatial management of invasive species: pathways and policy options. Environmental and Resource Economics 45 (4), 517–535.

Shapiro, A., 2003. Monte carlo sampling methods. Handbooks in Operations Research and Management Science 10, 353–425.

Shapiro, A., Dentcheva, D., Ruszczyński, A., 2014. Lectures on stochastic programming: modeling and theory, Second Editon. Society for Industrial and Applied Mathematics: Philadelphia.

Sharov, A. A., 2004. Bioeconomics of managing the spread of exotic pest species with barrier zones. Risk Analysis 24 (4), 879–892.

Sheldon, D., Dilkina, B., Elmachtoub, A., Finseth, R., Sabharwal, A., Conrad, J., Gomes, C., Shmoys, D., Allen, W., Amundsen, O., Vaughan, W., 2010. Maximizing the spread of cascades using network design. In: Proceedings of the Twenty-Sixth Conference Annual Conference on Uncertainty in Artificial Intelligence (UAI-10). AUAI Press, Corvallis, Oregon, pp. 517–526.

Shigesada, N., Kawasaki, K., 1997. Biological invasions: theory and practice. Oxford university press: Oxford.

Sinden, J., Jones, R., Hester, S., Odom, D., Kalisch, C., James, R., Cacho, O., Griffith, G., 2004. The economic impact of weeds in Australia. CRC for Australian Weed Management Technical Series No. 8. Available at `https://www.cbd.int/financial/values/australia-economicweeds.pdf` [Accessed: 25 June 2015].

Sivinski, J., Jeronimo, F., Holler, T., 2000. Development of aerial releases of diachasmimorpha tryoni (cameron) (hymenoptera: Braconidae), a parasitoid that attacks the mediterranean fruit fly, ceratitis capitata (weidemann) (diptera: Tephritidae), in the guatemalan highlands. Biocontrol Science and Technology 10 (1), 15–25, cited By 24.
URL `https://www.scopus.com/inward/record.uri?eid=2-s2.0-0034095955&doi=10.1080%2f09583150029341&partnerID=40&md5=5bd650525fca10d6de7eccd5b19e0956`

Tildesley, M. J., Savill, N. J., Shaw, D. J., Deardon, R., Brooks, S. P., Woolhouse, M. E. J., Grenfell, B. T., Keeling, M. J., Mar. 2006. Optimal reactive vaccination strategies for a foot-and-mouth outbreak in the UK. Nature 440 (7080), 83–86.

Tomassen, F., de Koeijer, A., Mourits, M., Dekker, A., Bouma, A., Huirne, R., 2002. A decision-tree to optimise control measures during the early stage of a foot-and-mouth disease epidemic. Preventive Veterinary Medicine 54 (4), 301 – 324.

Underwood, R., 2007. Fruit fly: Likely impact of an incursion of fruit fly in the bay of Plenty, Hawkes bay or Nelson. Fruition Horticulture (BOP) Ltd.

Verweij, B., Ahmed, S., Kleywegt, A., Nemhauser, G., Shapiro, A., 2003. The sample average approximation method applied to stochastic routing problems: A computational study. Computational Optimization and Applications 24 (2-3), 289–333.

Ward, M. P., Highfield, L. D., Vongseng, P., Garner, M. G., 2009. Simulation of foot-and-mouth disease spread within an integrated livestock system in Texas, USA. Preventive Veterinary Medicine 88 (4), 286–297.

Waterhouse, D. F., Sands, D. P. A., 2001. Classical biological control of arthropods in Australia. CSIRO Entomology Canberra.

White, B., Sadler, R., Florec, V., Dominiak, B., 2012. Economics of surveillance: a bioeconomic assessment of Queensland Fruit Fly. Contributed paper prepared for presentation at the 56th AARES annual conference, Fremantle, Western Australia, February 7-10, 2012.

Wilcove, D. S., Rothstein, D., Dubow, J., Phillips, A., Losos, E., 1998. Quantifying threats to imperiled species in the United States. BioScience 48 (8), 607–615.

Wilen, J. E., 2007. Economics of spatial-dynamic processes. American Journal of Agricultural Economics 89 (5), 1134–1144.

Williamson, M., 1996. Biological invasions. Population and Community Biology Series 15. Chapman and Hall: London.

World Bank, 2008. World Development Report: Agriculture for Development. World Bank: Washington DC.

Yonow, T., Sutherst, R. W., 1998. The geographical distribution of the Queensland fruit fly, Bactrocera (Dacus) tryoni, in relation to climate. Australian Journal of Agricultural Research 49 (6), 935–953.

Yonow, T., Zalucki, M., Sutherst, R., Dominiak, B., Maywald, G., Maelzer, D., Kriticos, D., 2004. Modelling the population dynamics of the Queensland fruit fly, Bactrocera (Dacus) tryoni: a cohort-based approach incorporating the effects of weather. Ecological Modelling 173 (1), 9 – 30.